

A reappraisal of the chemical composition of the Orion nebula based on VLT echelle spectrophotometry^{*}

C. Esteban,¹ M. Peimbert,² J. García-Rojas,¹ M.T. Ruiz,³
 A. Peimbert,² and M. Rodríguez,⁴

¹*Instituto de Astrofísica de Canarias, E-38200 La Laguna, Tenerife, Spain*

²*Instituto de Astronomía, UNAM, Apdo. Postal 70-264, México 04510 D.F., Mexico*

³*Departamento de Astronomía, Universidad de Chile, Casilla Postal 36D, Santiago de Chile, Chile*

⁴*Instituto Nacional de Astrofísica, Óptica y Electrónica INAOE, Apdo. Postal 51 y 216, 7200 Puebla, Pue., Mexico*

6 May 2019

ABSTRACT

We present VLT UVES echelle spectrophotometry of the Orion nebula in the 3100 to 10400 Å range. We have measured the intensity of 555 emission lines, many of them corresponding to permitted lines of different heavy-element ions. This is the largest set of spectral emission lines ever obtained for a Galactic or extragalactic H II region. We have derived He⁺, C⁺⁺, O⁺, O⁺⁺ and Ne⁺⁺ abundances from pure recombination lines. This is the first time that O⁺ and Ne⁺⁺ abundances are obtained from this kind of lines in the nebula. We have also derived abundances from collisionally excited lines for a large number of ions of different elements. In all cases, ionic abundances obtained from recombination lines are larger than those derived from collisionally excited lines. We have obtained remarkably consistent independent estimations of the temperature fluctuations parameter, t^2 , from different methods, which are also similar to other estimates from the literature. This result strongly suggests that moderate temperature fluctuations $-t^2$ between 0.02 and 0.03– are present in the Orion nebula. We have compared the chemical composition of the nebula with those of the Sun and other representative objects. The heavy element abundances in the Orion nebula are only slightly higher than the solar ones, a difference that can be explained by the chemical evolution of the solar vicinity.

Key words: ISM: abundances – H II regions – ISM: individual: Orion nebula.

1 INTRODUCTION

The Orion nebula is the brightest and nearest Galactic H II region in the sky and the most observed object of this kind. Our present-day knowledge about this remarkable nebula has been recently reviewed by O’Dell (2001) and Ferland (2001). The chemical composition of the Orion nebula has been traditionally considered the standard reference for the ionized gas in the solar neighborhood. Much work has been devoted to study the chemical abundances of this object (e.g., Peimbert & Torres-Peimbert 1977; Rubin et al. 1991; Baldwin et al. 1991, Osterbrock, Tran & Veilleux 1992; Esteban et al. 1998, hereinafter EPTE).

The analysis of the intensity ratios of collisionally excited lines (hereinafter CELs) has been the usual method

for determining the ionic abundances in ionized nebulae. Peimbert, Storey & Torres-Peimbert (1993) were the first in determining the O⁺⁺/H⁺ ratio from the intensity of the faint O II recombination lines (hereinafter RLs) in the Orion nebula. These authors find that the O⁺⁺/H⁺ ratio obtained from RLs is a factor of 2 larger than that derived from CELs. The RLs of heavy element ions that can be detected in the optical range are very faint, of the order of 10⁻³ or less of the intensity of H β . The brightest optical RLs in photoionized nebulae are those of C II λ 4267 Å and the multiplet 1 of O II around λ 4650 Å. The difference between the abundances determined from CELs and RLs (ofted called *abundance discrepancy*) can be of the order of 5 or even 20 for some planetary nebulae (see compilations by Rola & Stasińska 1994; Mathis & Liu 1999). In the case of H II regions the discrepancy seems to be present but not as large as in the case of the extreme planetary nebulae. Esteban et al. (1998, 1999a,b) have analyzed deep echelle spectra in several slit

^{*} Based on observations collected at the European Southern Observatory, Chile, proposal number ESO 68.C-0149(A)

positions of the Orion nebula, M17 and M8, determining C^{++} and O^{++} abundances (as well as the O^+ abundance in the case of M8) from CELs and RLs. The abundance discrepancies are similar for the different ions and slit positions for each nebula, reaching factors from 1.2 to 2.2. In more recent papers, Esteban et al. (2002), Peimbert (2003) and Tsamis et al. (2003) have estimated the abundance discrepancy for several extragalactic H II regions in M33, M101 and the Magellanic Clouds finding discrepancies rather similar to those found in the Galactic objects. These results are really puzzling, because a substantial part of our knowledge about the chemical composition of astronomical objects – and specially those in the extragalactic domain – is based on the analysis of CELs in ionized nebulae.

One of the most probable causes of the abundance discrepancy is the presence of spatial variations or fluctuations in the temperature structure of the nebulae (Peimbert 1967). Recent discussions and reviews about this problem can be found in Stasińska (2002), Liu (2002, 2003), Esteban (2002), and Torres-Peimbert & Peimbert (2003). The relation between both phenomena is possible due to the different functional dependence of the line emissivities of CELs and RLs on the electron temperature, which is stronger –exponential– in the case of CELs. Traditionally, following Peimbert’s formalism, the temperature fluctuations are parametrized by t^2 , the mean square temperature fluctuation of the gas. EPTE, Esteban et al. (1999a,b, 2002) and Peimbert (2003) have found that values of t^2 between 0.02 and 0.04 can account for the observed abundance discrepancy in the Galactic and extragalactic H II regions where RLs have been measured.

The main aim of this work is to make a reappraisal of the chemical composition of the Orion nebula in one of the slit positions observed by Peimbert & Torres-Peimbert (1977) and EPTE but including new echelle spectrophotometry obtained with the VLT. These new observations are described in the following section and give an unprecedentedly wider wavelength coverage for high-resolution spectroscopic observations of the Orion nebula. A total number of 555 lines are detected and measured, an important improvement with respect to the 220 lines observed by EPTE and the 444 ones identified –but partially analysed– by Baldwin et al. (2000). Abundance determinations of additional heavy element ions based on RLs, as O^+ , Ne^{++} or N^{++} are now possible, as well as abundance determinations of O^{++} and C^{++} based on additional lines not detected or identified in previous works.

2 OBSERVATIONS AND DATA REDUCTION

The observations were made on 2002 March 12 at Cerro Paranal Observatory (Chile), using the UT2 (Kueyen) of the Very Large Telescope (VLT) with the Ultraviolet Visual Echelle Spectrograph, UVES (D’Odorico et al. 2000). Two different settings –the standard ones– were used in both arms of the spectrograph covering from 3100 Å to 10400 Å. Some narrow spectral ranges could not be observed, 5783–5830 Å and 8540–8650 Å, due to the physical separation between the two CCDs of the detector system of the red arm, and 10084–10088 Å and 10252–10259 Å, because the last two orders of the spectrum do not fit within the size of the CCD.

Table 1. Journal of observations.

Date	$\Delta\lambda$ (Å)	Exp. time (s)
2002 March 12	3000–3900	5, 5×60
”	3800–5000	5, 5×120
”	4750–6800	5, 5×60
”	6700–10400	5, 5×120

The full width at half maximum (FWHM) of the spectral resolution at a given wavelength is $\Delta\lambda \approx \lambda/8800$. The slit position was chosen to cover approximately the same area of the Position 2 observed by EPTE. As in that previous work, the slit position was oriented east-west and centred at 25 arcsec South and 10 arcsec West of θ^1 Ori C, the brightest star of the Trapezium Cluster and the main ionizing source of the Orion nebula. The atmospheric dispersor corrector (ADC) was used during the observations to keep the same observed region within the slit independently of the change of the parallactic angle of the object during the night. The slit width was set to 3.0 arcsec as a compromise between the spectral resolution needed for the project and the desired signal-to-noise ratio of the spectra. The slit length was fixed to 10 arcsec in the blue arm and 12 arcsec in the red arm to avoid overlapping between consecutive orders in the spatial direction. Five individual exposures of 60 or 120 seconds were added to obtain the definitive spectra. Complementary shorter 5 seconds spectra were taken to obtain good intensity measurements for the brightest emission lines, which were close to saturation in the longer spectra. The one-dimensional spectra were extracted for an area of 3×8.5 arcsec².

The spectra were reduced using the IRAF¹ echelle reduction package following the standard procedure of bias subtraction, aperture extraction, flat-fielding, wavelength calibration and flux calibration. The correction for atmospheric extinction was performed using the average curve for the continuous atmospheric extinction at La Silla Observatory. The flux calibration was achieved by taking echellograms of the standard star EG 274. A journal of the observations is presented in Table 1.

3 LINE INTENSITIES AND REDDENING

Line intensities were measured integrating all the flux in the line between two given limits and over a local continuum estimated by eye. In the cases of evident line-blending, the line flux of each individual line was derived from a multiple Gaussian profile fit procedure. All these measurements were made with the SPLIT routine of the IRAF package.

All the line intensities of a given spectrum have been normalized to a particular non-saturated bright emission line present in each wavelength interval. For the bluest spectra (3000–3900 Å and 3800–5000 Å), the reference line was H 9 λ 3835 Å. In the case of the spectrum covering 4750–6800 Å the reference line was He I λ 5876 Å. Finally, the reference line for the reddest spectrum (6700–10400 Å) was [S II] λ 6731 Å. To produce a final homogeneous set of line

¹ IRAF is distributed by NOAO, which is operated by AURA, under cooperative agreement with NSF

Table 2. Observed and reddening-corrected line ratios [F(H β)=100] and identifications.

λ_0 (\AA)	Ion	Mult.	λ_{obs} (\AA)	$F(\lambda)$	$I(\lambda)$	err (%)
3187.84	He I	3	3187.92	1.691	2.796	8
3276.04	C II		3276.20	0.064	0.102	:
3296.77	He I	9	3296.93	0.085	0.135	30
3322.54	[Fe III] ?	5F	3322.68	0.044	0.069	31
3323.75	Ne II	7	3323.87	0.037	0.058	36
3324.87	S III	2	3325.01	0.047	0.074	29
3334.87	Ne II	2	3334.97	0.060	0.094	24
3354.42	He I	8	3354.72	0.135	0.210	13
3367.05	Ne II	12	3367.30	0.034	0.054	37
3367.22	Ne II	19				
3387.13	S III	2	3387.27	0.078	0.120	20
3388.46	Ne II	19	3388.57	0.020	0.030	:
3447.59	He I	7	3447.76	0.219	0.332	9
3450.39	[Fe II]	27F	3450.49	0.027	0.041	:
3453.07	Ne II	21	3453.51	0.015	0.023	:
	?		3454.82	0.013	0.020	:
3456.83	N II		3457.07	0.025	0.038	:
3461.01	Ca I] ?		3461.17	0.027	0.041	:
3465.94	He I		3466.12	0.024	0.036	:
3471.80	He I		3471.97	0.042	0.063	30
3478.97	He I	48	3479.14	0.041	0.062	25
3487.73	He I	42	3487.91	0.058	0.087	25
3498.66	He I	40	3498.84	0.075	0.112	20
3511.10	O I		3511.30	0.017	0.025	:
3512.52	He I	38	3512.69	0.092	0.137	17
3530.50	He I	36	3530.68	0.128	0.189	18
3536.80	He I		3536.93	0.010	0.015	:
3536.81	He I					
3536.93	He I					
3554.42	He I	34	3554.62	0.162	0.237	11
3587.28	He I	32	3587.47	0.234	0.340	9
3613.64	He I	6	3613.82	0.342	0.493	7
3631.95	[Fe III] ?		3632.16	0.025	0.036	:
3634.25	He I	28	3634.43	0.346	0.495	7
3651.97	He I	27	3652.16	0.017	0.024	:
3661.22	H I	H31	3661.41	0.204	0.290	9
3662.26	H I	H30	3662.43	0.250	0.355	8
3663.40	H I	H29	3663.59	0.236	0.335	8
3664.68	H I	H28	3664.86	0.247	0.350	9
3666.10	H I	H27	3666.29	0.292	0.414	7
3667.68	H I	H26	3667.87	0.336	0.475	7
3669.47	H I	H25	3669.66	0.375	0.531	6
3671.48	H I	H24	3671.67	0.412	0.583	6
3673.76	H I	H23	3673.95	0.447	0.632	6
3676.37	H I	H22	3676.56	0.519	0.733	6
3679.36	H I	H21	3679.55	0.588	0.830	6
3682.81	H I	H20	3683.00	0.644	0.908	5
3686.83	H I	H19	3687.02	0.684	0.962	5
3691.56	H I	H18	3691.75	0.802	1.127	4
3694.22	Ne II	1	3694.39	0.030	0.042	30
3697.15	H I	H17	3697.34	0.960	1.347	4
3703.86	H I	H16	3704.04	1.090	1.527	4
3705.04	He I	25	3705.20	0.513	0.717	5
3709.37	S III	1	3709.67	0.035	0.048	:
3711.97	H I	H15	3712.16	1.303	1.820	4
3712.74	O II	3	3712.85	0.025	0.035	:
3713.08	Ne II	5	3713.23	0.033	0.046	:
3717.72	S III	6	3717.92	0.059	0.083	24
3721.83	[S III]	2F	3722.04	2.481	3.453	4
3721.94	H I	H14				

Table 2. –continued

λ_0 (\AA)	Ion	Mult.	λ_{obs} (\AA)	$F(\lambda)$	$I(\lambda)$	err (%)
3726.03	[O II]	1F	3726.30	40.122	55.776	4
	?		3727.40	0.055	0.076	:
3728.82	[O II]	1F	3729.04	19.366	26.898	4
3732.86	He I	24	3733.06	0.037	0.052	:
3734.37	H I	H13	3734.56	1.929	2.675	4
3737.55	Ne II		3737.85	0.018	0.025	:
3749.48	O II	3	3749.62	0.083	0.115	18
3750.15	H I	H12	3750.34	2.377	3.280	4
3756.10	He I		3756.32	0.043	0.060	31
3768.78	He I		3768.99	0.015	0.020	:
	?		3769.95	0.017	0.023	:
3770.63	H I	H11	3770.82	3.058	4.193	4
3784.89	He I	64	3785.07	0.027	0.036	:
3786.72	[Cr II]		3786.90	0.011	0.016	:
3787.40	He I		3787.61	0.006	0.009	:
3797.63	[S III]	2F	3798.10	3.969	5.394	3
3797.90	H I	H10				
3805.74	He I	58	3805.96	0.041	0.055	22
3806.54	Si III	5	3806.68	0.017	0.023	30
3819.61	He I	22	3819.82	0.899	1.213	3
3829.77	Ne II	39	3829.92	0.013	0.018	:
3831.66	S II		3831.87	0.038	0.051	12
3833.57	He I		3833.73	0.043	0.058	11
3835.39	H I	H9	3835.58	5.407	7.264	3
3837.73	S III	5	3837.91	0.022	0.029	18
3838.09	He I	61	3838.47	0.048	0.064	10
3838.37	N II	30				
3853.66	Si II	1	3853.90	0.021	0.029	:
3856.02	Si II	1	3856.27	0.146	0.195	6
3856.13	O II	12				
3860.64	S II	50	3860.81	0.019	0.026	19
3862.59	Si II	1	3862.83	0.076	0.102	9
3864.12	O II	11	3864.54	0.021	0.027	:
3867.49	He I	20	3867.69	0.060	0.080	9
3868.75	[Ne III]	1F	3868.94	17.203	22.870	3
3871.82	He I	60	3871.97	0.067	0.089	8
3878.18	He I		3878.39	0.012	0.016	:
3882.19	O II	12	3882.41	0.016	0.021	:
3888.65	He I	2	3889.18	11.380	15.032	3
3889.05	H I	H8				
3918.98	C II	4	3919.12	0.052	0.068	10
3920.68	C II	4	3920.83	0.109	0.143	6
3926.53	He I	58	3926.75	0.095	0.124	7
3928.55	S III		3928.74	0.017	0.022	18
3935.94	He I	57	3936.18	0.017	0.022	:
3954.36	O II	6	3954.72	0.019	0.025	:
3964.73	He I	5	3964.93	0.740	0.954	3
3967.46	[Ne III]	1F	3967.64	5.314	6.849	3
3970.07	H I	H7	3970.27	12.366	15.925	3
3973.24	O II	6	3973.45	0.016	0.020	35
3983.72	S III	8	3983.97	0.032	0.040	15
3985.93	S III	8	3986.12	0.021	0.027	18
3993.06	[Ni II]		3993.46	0.013	0.017	25
3994.99	N II	12	3995.18	0.008	0.010	:
4004.15	Fe II ?		4004.24	0.024	0.031	:
4008.36	[Fe III]	4F	4008.57	0.017	0.022	21
4009.22	He I	55	4009.46	0.134	0.171	5
4023.98	He I	54	4024.19	0.017	0.021	22
4026.08	N II	40	4026.41	1.722	2.181	3
4026.21	He I	18				

Table 2. –*continued*

λ_0 (Å)	Ion	Mult.	λ_{obs} (Å)	$F(\lambda)$	$I(\lambda)$	err (%)
	?		4027.42	0.025	0.031	16
4041.31	N II	39	4041.49	0.010	0.013	:
4060.60	O II	97	4060.80	0.003	0.004	:
4062.94	O II	50	4063.18	0.005	0.006	:
4068.60	[S II]	1F	4068.92	1.112	1.392	3
4069.62	O II	10	4069.98	0.069	0.086	8
4069.89	O II	10				
4072.15	O II	10	4072.34	0.054	0.067	9
4075.86	O II	10	4076.06	0.063	0.079	8
4076.35	[S II]	1F	4076.67	0.372	0.464	3
4078.84	O II	10	4079.05	0.009	0.011	:
4083.90	O II	47	4084.07	0.008	0.010	37
4085.11	O II	10	4085.32	0.011	0.013	30
4087.15	O II	48	4087.36	0.010	0.013	31
4089.29	O II	48	4089.49	0.020	0.025	19
4092.93	O II	10	4093.11	0.008	0.010	:
4095.64	O II	48	4095.82	0.005	0.007	:
4097.22	O II	20	4097.47	0.038	0.047	10
4097.26	O II	48				
4101.74	H I	H6	4101.95	20.231	25.090	2
4104.99	O II	20	4105.12	0.019	0.024	19
4107.09	O II	48.01	4107.25	0.004	0.006	:
4110.79	O II	20	4110.94	0.019	0.024	19
4112.10	Ne I		4112.25	0.006	0.008	:
4114.48	[Fe II]	23F	4114.78	0.005	0.006	:
4116.07	Fe II ?		4116.22	0.006	0.007	:
4119.22	O II	20	4119.41	0.025	0.031	16
4120.82	He I	16	4121.01	0.179	0.221	4
4121.46	O II	19	4121.63	0.033	0.041	13
4129.32	O II	19	4129.48	0.006	0.008	:
4131.89	[Fe III]		4131.94	0.013	0.016	30
4132.80	O II	19	4132.98	0.027	0.033	15
4143.76	He I	53	4143.96	0.233	0.285	4
4145.90	O II	106	4146.31	0.011	0.014	29
4146.08	O II	106				
4153.30	O II	19	4153.47	0.062	0.076	8
4156.36	N II	19	4156.53	0.059	0.072	9
4168.97	He I	52	4169.28	0.049	0.060	10
4185.45	O II	36	4185.65	0.017	0.021	21
4189.79	O II	36	4189.96	0.021	0.025	18
4201.35	N II	49	4201.59	0.005	0.006	:
4219.76	Ne II	52	4219.92	0.007	0.008	:
4236.91	N II	48	4237.25	0.006	0.007	:
4237.05	N II	48				
4241.78	N II	48	4241.97	0.010	0.012	:
4242.49	N II	48	4242.80	0.010	0.012	:
4243.97	[Fe II]	21F	4244.37	0.035	0.042	12
4249.08	[Fe II]		4249.25	0.006	0.008	:
4253.54	S III	4	4253.79	0.035	0.041	13
4267.15	C II	6	4267.38	0.201	0.238	4
4275.55	O II	67	4275.76	0.014	0.017	24
4276.75	O II	67	4277.20	0.027	0.032	15
4276.83	[Fe II]	21F				
4287.39	[Fe II]	7F	4287.79	0.065	0.087	8
4294.78	S II	49	4294.83	0.015	0.018	23
4294.92	O II	54				
4300.66	Fe II ?		4300.81	0.055	0.065	9
4303.82	O II	53	4304.02	0.014	0.017	24
4303.82	O II	53				
4307.23	O II	54	4307.43	0.006	0.007	:
4317.14	O II	2	4317.31	0.038	0.044	12
4319.63	O II	2	4319.84	0.022	0.025	18

Table 2. –*continued*

λ_0 (Å)	Ion	Mult.	λ_{obs} (Å)	$F(\lambda)$	$I(\lambda)$	err (%)
4325.76	O II	2	4325.95	0.014	0.017	24
4326.40	O I		4326.66	0.026	0.031	15
4326.24	[Ni II]	2D-4P				
4332.69	O II	65	4332.90	0.018	0.020	21
4336.79	[Cr II]	a6D-a2	4337.04	0.019	0.022	19
4340.47	H I	H γ	4340.69	38.720	44.932	2
4344.35	O I ?		4344.53	0.005	0.006	:
4345.55	O II	63.01	4345.72	0.055	0.064	9
4345.56	O II	2				
4346.85	[Fe II]	21F	4347.42	0.013	0.015	:
4349.43	O II	2	4349.62	0.056	0.065	9
4351.26	O II	16	4351.46	0.007	0.008	:
4352.78	[Fe II]	21F	4353.17	0.010	0.012	25
4359.34	[Fe II]	7F	4359.74	0.050	0.058	10
4361.54	S III	4	4361.73	0.014	0.016	25
4363.21	[O III]	2F	4363.42	1.129	1.301	2
4364.61	Mn II ?		4364.86	0.005	0.005	:
4366.89	O II	2	4367.06	0.042	0.048	11
4368.19	O I	5	4368.66	0.063	0.073	9
4368.25	O I	5				
4375.72	Ne I		4376.12	0.008	0.009	:
4387.93	He I	51	4388.15	0.473	0.542	2
4391.94	Ne II	57	4392.14	0.012	0.014	27
4409.30	Ne II	57	4409.50	0.008	0.009	36
4413.78	[Fe II]	7F	4414.19	0.036	0.036	13
4414.90	O II	5	4415.09	0.032	0.036	16
4416.27	[Fe II]	6F	4416.67	0.040	0.045	14
4416.97	O II	5	4417.16	0.024	0.028	16
4422.36	Ni II ?		4422.51	0.005	0.005	:
4422.37	Cr II ?					
4428.54	Ne II	57	4428.71	0.008	0.009	:
4432.51	Ne I		4432.76	0.009	0.010	:
4432.54	Ne I					
4437.55	He I	50	4437.78	0.063	0.071	8
4452.11	[Fe II]	7F	4452.51	0.029	0.033	14
4452.38	O II	5				
4457.95	[Fe II]	6F	4458.37	0.017	0.020	21
4465.41	O II	94	4465.67	0.015	0.017	23
4467.92	O II	94	4468.15	0.008	0.009	:
4471.09	He I	14	4471.72	4.042	4.523	1
4474.91	[Fe II]	7F	4475.32	0.012	0.013	28
4491.14	[Fe IV]		4491.45	0.009	0.010	33
4492.64	[Fe II]	6F	4493.07	0.009	0.010	34
4514.90	[Fe II]	6F	4515.26	0.007	0.008	:
4571.20	Mg I	1	4571.44	0.005	0.005	:
4590.97	O II	15	4591.18	0.023	0.025	17
4592.43	Fe I ?		4592.62	0.005	0.005	:
4595.95	O II	15	4596.38	0.019	0.020	20
4596.18	O II	15				
4596.83	[Ni III]		4597.26	0.005	0.005	:
4601.48	N II	5	4601.69	0.012	0.013	27
4602.11	O II	93	4602.34	0.005	0.006	:
4607.16	N II	5	4607.37	0.039	0.042	12
4607.13	[Fe III]	3F				
4609.44	O II	93	4609.68	0.012	0.013	27
4613.87	N II	5	4614.07	0.010	0.010	32
4620.11	C II ?		4620.83	0.015	0.016	24
4620.26	C II ?					
4621.39	N II	5	4621.62	0.015	0.016	24
4628.05	[Ni II]		4628.49	0.006	0.007	:
4630.54	N II	5	4630.76	0.044	0.048	10

Table 2. –continued

λ_0 (Å)	Ion	Mult.	λ_{obs} (Å)	$F(\lambda)$	$I(\lambda)$	err (%)
4634.14	N III	2	4634.31	0.016	0.018	22
4638.86	O II	1	4639.05	0.053	0.057	9
4640.64	N III	2	4640.80	0.027	0.029	13
4641.81	O II	1	4642.02	0.096	0.102	5
4641.85	N III	2				
4643.06	N II	5	4643.31	0.014	0.015	25
4649.13	O II	1	4649.35	0.146	0.155	3
4650.84	O II	1	4651.04	0.049	0.052	10
4658.10	[Fe III]	3F	4658.42	0.517	0.549	2
4661.63	O II	1	4661.81	0.064	0.068	8
4667.01	[Fe III]	3F	4667.25	0.029	0.031	14
4673.73	O II	1	4673.99	0.011	0.011	29
4676.24	O II	1	4676.43	0.033	0.035	13
4696.36	O II	1	4696.60	0.004	0.004	:
4699.22	O II	25	4699.39	0.010	0.010	32
4701.62	[Fe III]	3F	4701.88	0.165	0.172	4
4705.35	O II	25	4705.57	0.018	0.018	21
4710.07	Ne I	11	4710.23	0.007	0.007	:
4711.37	[Ar IV]	1F	4711.56	0.096	0.100	6
4713.14	He I	12	4713.41	0.657	0.685	1
4728.07	[Fe II]	4F	4728.45	0.005	0.005	:
4733.93	[Fe III]	3F	4734.20	0.066	0.069	8
4740.16	[Ar IV]	1F	4740.42	0.116	0.121	5
4752.95	O II		4753.15	0.010	0.010	31
4754.83	[Fe III]	3F	4755.05	0.100	0.103	6
4769.6	[Fe III]	3F	4769.77	0.060	0.061	8
4772.18	Cr II ?		4772.46	0.005	0.006	:
4774.74	[Fe II]	20F	4775.16	0.009	0.010	33
4777.88	[Fe III]	3F	4778.02	0.032	0.033	11
4779.71	N II	20	4779.99	0.011	0.011	29
4788.13	N II	20	4788.37	0.014	0.014	25
4802.36	[Co II] ?		4802.75	0.011	0.011	29
4803.29	N II	20	4803.55	0.018	0.019	20
4814.55	[Fe II]	20F	4815.00	0.040	0.041	11
4815.51	S II	9	4815.84	0.016	0.016	22
4861.33	H I	H β	4861.61	100.000	100.000	0.7
4881.00	[Fe III]	2F	4881.40	0.255	0.254	3
4889.70	[Fe II]		4890.11	0.026	0.026	15
4890.86	O II	28	4891.09	0.022	0.022	19
4895.05	N I	78	4895.21	0.015	0.015	24
4902.65	Si II	7.23	4902.91	0.014	0.013	25
4905.34	[Fe II]	20F	4905.88	0.016	0.015	23
4921.93	He I	48	4922.23	1.240	1.222	1
4924.50	[Fe III]	2F	4924.76	0.050	0.049	10
4924.53	O II	28				
4930.50	[Fe III]	1F	4930.98	0.021	0.021	18
4931.32	[O III]	1F	4931.53	0.053	0.052	9
4943.04	O II	33	4943.41	0.010	0.010	:
4947.38	[Fe II]	20F	4947.86	0.008	0.008	:
4949.39	Ar II ?		4949.54	0.007	0.007	:
4958.91	[O III]	1F	4959.22	131.389	128.202	0.7
4968.63	Cr II		4968.94	0.010	0.010	:
4980.13	O I		4980.42	0.013	0.012	26
4985.90	[Fe III]	2F	4986.15	0.012	0.012	27
4987.20	[Fe III]	2F	4987.62	0.047	0.046	10
4987.38	N II	24				
4994.37	N II	24	4994.74	0.018	0.018	35
4997.02	MnII ?		4997.28	0.036	0.035	18
5001.13	N II	19	5001.72	0.031	0.030	16
5001.47	N II	19				
5006.84	[O III]	1F	5007.19	398.147	383.804	0.7
5011.30	[Fe III]	1F	5011.72	0.070	0.067	14

Table 2. –continued

λ_0 (Å)	Ion	Mult.	λ_{obs} (Å)	$F(\lambda)$	$I(\lambda)$	err (%)
5015.68	He I	4	5016.02	2.397	2.306	1
	?		5017.14	0.025	0.024	20
5035.49	[Fe II]	4F	5036.16	0.020	0.019	24
5041.03	Si II	5	5041.40	0.118	0.113	7
5041.98	O II	23.01	5042.32	0.026	0.024	19
5045.10	N II	4	5045.44	0.015	0.014	20
5047.74	He I	47	5048.33	0.605	0.577	2
5055.98	Si II	5	5056.40	0.207	0.197	4
5084.77	[Fe III]	1F	5085.11	0.012	0.011	35
5111.63	[Fe II]	19F	5112.25	0.019	0.018	25
5121.82	C II	12	5122.16	0.010	0.009	:
5146.61	O I		5147.25	0.040	0.037	15
5146.61	O I					
5158.81	[Fe II]	19F	5159.37	0.064	0.060	9
5191.82	[Ar III]	3F	5192.07	0.072	0.066	9
5197.90	[N I]	1F	5198.50	0.140	0.128	6
5200.26	[N I]	1F	5200.85	0.083	0.076	8
5219.31	S III		5219.71	0.011	0.010	38
5261.61	[Fe II]	19F	5262.21	0.052	0.047	11
5270.40	[Fe III]	1F	5270.93	0.305	0.274	2
5273.38	[Fe II]	18F	5273.92	0.023	0.021	21
5274.97	O I	27	5275.69	0.013	0.011	30
5275.12	O I	27				
5298.89	O I	26	5299.60	0.031	0.028	17
5299.04	O I	26				
5342.40	C II	17.06	5342.73	0.015	0.013	30
5363.35	[Ni IV]	4F-2G	5363.94	0.009	0.008	:
5405.15	Ne II		5405.30	0.008	0.007	:
5412.00	[Fe III]	1F	5412.53	0.030	0.026	17
5433.49	O II		5433.71	0.008	0.007	:
5453.81	S II	6	5454.24	0.012	0.010	:
5495.67	N II	29	5495.98	0.006	0.005	:
5512.77	O I	25	5513.32	0.028	0.024	18
5517.71	[Cl III]	1F	5518.03	0.454	0.383	3
5537.88	[Cl III]	1F	5538.20	0.704	0.590	2
5551.95	N II	63	5552.30	0.009	0.007	:
5554.83	O I	24	5555.55	0.030	0.025	17
5555.03	O I	24				
5577.34	[O I]	3F	5577.89	0.010	0.008	:
5666.64	N II	3	5666.93	0.035	0.029	15
5676.02	N II	3	5676.35	0.012	0.010	:
5679.56	N II	3	5679.92	0.053	0.043	11
5686.21	N II	3	5686.59	0.008	0.006	:
5710.76	N II	3	5711.06	0.011	0.009	35
5739.73	Si III	4	5740.05	0.047	0.037	12
5746.96	[Fe II]	34F	5747.59	0.006	0.005	:
	?		5752.86	0.007	0.006	:
5754.64	[N II]	3F	5755.08	0.858	0.680	3
5867.99	Ni II ?		5868.26	0.026	0.020	30
5875.64	He I	11	5875.98	18.764	14.418	3
5906.15	Si I ?		5906.35	0.011	0.008	:
5927.82	N II	28	5928.16	0.013	0.010	:
5931.78	N II	28	5932.15	0.026	0.020	19
5941.65	N II	28	5941.91	0.020	0.015	24
5944.38	Fe II ?		5944.70	0.007	0.005	:
5944.40	Fe II ?					
5952.39	N II	28	5952.80	0.017	0.012	:
5957.56	Si II	4	5958.09	0.061	0.046	10
5958.39	O I	23	5959.19	0.050	0.038	12
5958.58	O I	23				
5978.93	Si II	4	5979.43	0.130	0.097	6
6000.20	[Ni III]	2F	6000.59	0.015	0.011	30
6046.23	O I	22	6046.99	0.121	0.089	7

Table 2. –*continued*

λ_0 (Å)	Ion	Mult.	λ_{obs} (Å)	$F(\lambda)$	$I(\lambda)$	err (%)
6046.44	O I	22				
6046.49	O I	22				
6151.43	C II	16.04	6151.73	0.012	0.009	36
6155.98	O I	10	6156.27	0.008	0.005	:
6157.42	Ni II		6157.68	0.008	0.006	:
6256.83	O I	50.01	6257.42	0.016	0.011	28
6300.30	[O I]	1F	6300.91	1.049	0.707	5
6312.10	[S III]	3F	6312.44	2.762	1.853	4
6347.11	Si II	2	6347.55	0.266	0.176	5
6363.78	[O I]	1F	6364.39	0.368	0.242	5
6365.10	[Ni II]	8F	6365.72	0.014	0.009	32
6371.36	Si II	2	6371.76	0.149	0.098	7
6401.4	[Ni III]	2F	6401.70	0.010	0.007	:
6402.25	Ne I	1	6402.77	0.013	0.009	:
6454.77	C II	17.05	6455.33	0.008	0.005	:
6461.95	C II	17.04	6462.23	0.039	0.025	15
6533.8	[Ni III]	2F	6533.99	0.037	0.023	15
6548.03	[N II]	1F	6548.57	19.665	12.201	5
6552.62	Cr II ?		6553.00	0.024	0.015	:
6555.84	O II	105.39	6556.11	0.012	0.008	:
6562.82	H I	H α	6563.15	465.402	287.378	5
6576.48	O II		6576.71	0.013	0.008	33
6576.57	O II					
6578.05	C II	2	6578.36	0.473	0.291	6
6583.41	[N II]	1F	6583.94	61.589	37.769	5
6666.80	[Ni II]	8F	6667.44	0.024	0.014	21
6678.15	He I	46	6678.49	6.475	3.848	6
6682.2	[Ni III]	2F	6682.23	0.008	0.005	:
6710.97	[Fe II]		6711.03	0.005	0.003	:
6716.47	[S II]	2F	6716.96	3.303	1.938	6
6721.39	O II	4	6721.71	0.011	0.006	:
6730.85	[S II]	2F	6731.36	6.023	3.518	6
6734.00	C II	21	6734.42	0.010	0.006	:
6739.8	[Fe IV]		6740.23	0.009	0.005	:
6744.39	N II		6744.42	0.006	0.003	:
6747.5	[Cr IV] ?		6747.97	0.007	0.004	34
6755.85	He I	1/20	6756.28	0.006	0.003	32
6755.9	[Fe IV]					
6759.14	[Cr II]		6759.40	0.004	0.002	:
6760.78	MnII ?		6760.98	0.004	0.002	:
6769.59	N I	58	6769.97	0.009	0.005	29
6785.81	O II		6786.05	0.009	0.005	27
6787.04	Fe II ?		6787.41	0.003	0.001	:
6791.48	[Ni II]	8F	6791.97	0.012	0.007	22
6797.00	[Ni III]		6797.12	0.005	0.003	:
?			6809.88	0.007	0.004	34
6809.99	N II	54	6810.46	0.004	0.003	:
6813.57	[Ni II]	8F	6814.23	0.008	0.005	23
6818.42	Si II		6818.75	0.003	0.002	:
6821.16	[Mn III] ?		6821.68	0.003	0.002	:
6855.88	He I	1/12	6856.34	0.016	0.009	18
6933.91	He I		6934.29	0.025	0.014	14
6989.47	He I		6989.89	0.024	0.013	12
7001.92	O I	21	7002.80	0.161	0.086	8
7002.23	O I	21				
7047.13	Fe II ?		7047.31	0.010	0.006	25
7062.26	He I	1/11	7062.65	0.037	0.019	10
7065.28	He I	10	7065.58	14.162	7.398	7
7096.99	S II ?		7097.22	0.011	0.006	24
7097.12	Si I					
7110.90	[Cl IV]		7111.12	0.005	0.002	:
7113.42	Si II	7.19	7113.66	0.004	0.002	:

Table 2. –*continued*

λ_0 (Å)	Ion	Mult.	λ_{obs} (Å)	$F(\lambda)$	$I(\lambda)$	err (%)
7115.63	C II	20	7115.92	0.006	0.003	:
7135.78	[Ar III]	1F	7136.13	31.779	16.197	7
7151.08	O II	99.01	7151.39	0.006	0.003	:
7155.14	[Fe II]	14F	7155.82	0.085	0.043	9
7160.13	He I	1/10	7160.89	0.055	0.028	10
7231.34	C II	3	7231.62	0.148	0.073	9
7236.42	C II	3	7236.82	0.494	0.243	8
7243.99	[Ni I]	2F	7244.30	0.041	0.020	12
7254.15	O I	20	7255.06	0.216	0.106	8
7254.45	O I	20				
7254.53	O I	20				
7281.35	He I	45	7281.74	1.231	0.597	8
7298.05	He I	1/9	7298.37	0.077	0.037	10
7318.39	[O II]	2F	7320.45	11.363	5.432	8
7319.99	[O II]	2F				
7329.66	[O II]	2F	7330.78	8.721	4.154	8
7330.73	[O II]	2F				
7377.83	[Ni II]	2F	7378.54	0.152	0.071	9
7388.16	[Fe II]	14F	7388.82	0.015	0.007	20
7411.61	[Ni II]	2F	7412.34	0.048	0.022	10
7423.64	N I	3	7424.36	0.027	0.012	15
7442.30	N I	3	7443.04	0.067	0.031	10
7452.54	[Fe II]	14F	7453.22	0.033	0.015	13
7459.30	[V II] ?	4F	7459.64	0.005	0.002	:
7468.31	N I	3	7469.03	0.096	0.044	10
7499.85	He I	1/8	7500.21	0.122	0.055	10
7504.94	O II		7505.33	0.014	0.006	21
7519.49	C II	16.08	7520.09	0.018	0.008	18
7519.86	C II	16.08				
7530.57	C II	16.08	7530.76	0.046	0.020	12
7535.21	N II ?		7535.32	0.008	0.004	36
7745.10	Si I ?		7745.47	0.008	0.003	:
7751.10	[Ar III]	2F	7751.50	8.949	3.682	10
7771.94	O I	1	7772.55	0.040	0.016 ^a	:
7775.39	O I	1	7775.95	0.013	0.006	21
7811.68	He I		7812.05	0.009	0.003	29
7816.13	He I	1/7	7816.52	0.197	0.079	10
7876.03	[P II] ?		7876.59	0.014	0.005	22
7890.07	Ca I]		7890.50	0.096	0.038	11
7937.13	He I	4/27	7937.61	0.006	0.002	:
7971.62	He I	2/11	7972.09	0.011	0.004	25
?	?		7973.58	0.008	0.003	30
7982.40	O I	19	7982.78	0.006	0.002	:
7987.33	O I	19	7987.82	0.011	0.004	32
8000.08	[Cr II]	1F	8000.81	0.029	0.011	16
8015.67	Ca I]		8016.22	0.005	0.002	:
8030.65	Ca I]		8031.25	0.011	0.004	:
8034.9	Si I		8035.30	0.009	0.003	:
8045.62	[Cl IV]	1F	8046.05	0.109	0.041	12
8057	He I	4/18	8057.97	0.012	0.005	24
8084	He I	4/17	8084.73	0.007	0.002	:
8092.53	Ca I]		8092.97	0.007	0.002	:
8094.08	He I	4/10	8094.50	0.014	0.005	22
8116	He I	4/16	8116.81	0.015	0.006	21
8125.31	Ca I]		8126.02	0.014	0.005	22
8155.66	He I		8155.93	0.021	0.008	18
8200.36	N I	2	8201.17	0.027	0.010	16
8203.85	He I	4/14	8204.31	0.026	0.009	17
8210.72	N I	2	8211.72	0.009	0.003	29
8216.34	N I	2	8217.02	0.073	0.026	13
8223.14	N I	2	8223.95	0.149	0.053	12
8245.64	H I	P42	8246.06	0.105	0.037	12

Table 2. –continued

λ_0 (Å)	Ion	Mult.	λ_{obs} (Å)	$F(\lambda)$	$I(\lambda)$	err (%)
8247.73	H I	P41	8248.16	0.117	0.041	12
8249.20	H I	P40	8250.42	0.125	0.044	12
8252.40	H I	P39	8252.83	0.129	0.046	12
8255.02	H I	P38	8255.27	0.076	0.027	13
8257.85	H I	P37	8258.24	0.137	0.048	12
8260.93	H I	P36	8261.36	0.173	0.061	12
8264.28	H I	P35	8264.76	0.207	0.073	12
8267.94	H I	P34	8268.37	0.182	0.064	12
8271.93	H I	P33	8272.35	0.199	0.070	12
8276.31	H I	P32	8276.85	0.268	0.094	12
8281.12	H I	P31	8281.63	0.181	0.063	12
8286.43	H I	P30	8286.71	0.161	0.056	12
8292.31	H I	P29	8292.70	0.272	0.095	12
8298.83	H I	P28	8299.17	0.261	0.091	12
8306.11	H I	P27	8306.54	0.336	0.117	12
8314.26	H I	P26	8314.66	0.368	0.128	12
8323.42	H I	P25	8323.86	0.435	0.151	12
	?		8330.35	0.019	0.007	19
8333.78	H I	P24	8334.21	0.453	0.157	12
8342.33	He I	4/12	8342.61	0.068	0.023	13
8345.55	H I	P23	8345.99	0.511	0.176	12
8359.00	H I	P22	8359.43	0.601	0.207	12
8361.67	He I	1/6	8362.14	0.336	0.115	12
8374.48	H I	P21	8374.91	0.636	0.217	12
8376	He I	6/20	8376.98	0.021	0.007	18
8392.4	H I	P20	8392.84	0.713	0.243	12
8397	He I	6/19	8397.68	0.024	0.008	17
8413.32	H I	P19	8413.79	0.891	0.302	12
8422	He I	6/18	8422.41	0.029	0.010	16
8424	He I	7/18	8424.66	0.015	0.005	22
8433.94	[Cl III]	3F	8434.09	0.027	0.009	17
8437.96	H I	P18	8438.39	0.981	0.330	12
8446.25	O I	4	8447.28	2.626	0.882	12
8446.36	O I	4				
8446.76	O I	4				
8453.15	Fe I] ?		8453.85	0.019	0.006	19
8453.66	Fe I] ?					
8459.50	Ca I]		8459.98	0.005	0.002	:
8467.25	H I	P17	8467.69	1.123	0.375	12
8476.98	Ni II ?		8477.45	0.013	0.004	:
8480.90	[Cl III]	3F	8481.28	0.031	0.010	16
8486.27	He I	6/16	8486.70	0.040	0.013	15
8488.73	He I	7/16	8489.15	0.015	0.005	22
8488.77	He I	5/16				
8499.7	[Cl III]	3F	8500.33	0.082	0.027	13
8502.48	H I	P16	8502.96	1.400	0.463	12
8518.04	He I	2/8	8518.40	0.030	0.010	19
8528.99	He I	6/15	8529.44	0.060	0.020	16
8531.48	He I	7/15	8532.09	0.025	0.008	18
8665.02	H I	P13	8665.44	2.489	0.789	13
8680.28	N I	1	8681.04	0.105	0.033	14
8683.40	N I	1	8684.24	0.091	0.029	14
8686.15	N I	1	8686.91	0.078	0.025	14
8703.25	N I	1	8704.13	0.067	0.021	14
8711.70	N I	1	8712.54	0.069	0.022	14
8718.83	N I	1	8719.65	0.042	0.013	15
8727.13	[C I]	3F	8727.90	0.053	0.017	15
8728.90	[Fe III]	8F	8729.83	0.036	0.011	16
8728.90	N I	21				
8733.43	He I	6/12	8733.87	0.107	0.033	14
8736.04	He I	7/12	8736.48	0.036	0.011	16
8739.97	He I	5/12	8740.51	0.011	0.003	27
8750.47	H I	P12	8750.93	3.175	0.985	13

Table 2. –continued

λ_0 (Å)	Ion	Mult.	λ_{obs} (Å)	$F(\lambda)$	$I(\lambda)$	err (%)
8776.77	He I	4/9	8777.39	0.260	0.080	13
8816.82	He I	10/12	8817.08	0.017	0.005	21
8820.00	Fe II] ?		8820.38	0.007	0.002	:
8829.40	[S III]	3F	8830.21	0.042	0.013	16
8831.87	[Cr II]	18F	8832.21	0.017	0.005	:
8838.2	[Fe III]		8838.75	0.009	0.003	29
8845.38	He I	6/11	8845.82	0.153	0.046	14
8848.05	He I	7/11	8848.80	0.108	0.033	14
8854.11	He I	5/11	8854.51	0.027	0.008	18
8862.79	H I	P11	8863.24	4.133	1.245	13
8892.22	Ne I		8892.72	0.035	0.011	16
8914.77	He I	2/7	8915.18	0.064	0.019	15
8930.97	He I	10/11	8931.16	0.017	0.005	22
8996.99	He I	6/10	8997.42	0.199	0.058	14
9014.91	H I	P10	9015.24	3.320	0.963	14
9015.77	N II ?		9016.42	0.077	0.022	15
9052.16	Ca I]		9052.85	0.018	0.005	:
9063.29	He I	4/8	9063.78	0.179	0.052	14
	?		9067.72	0.031	0.009	17
9068.90	[S III]	1F	9069.42	105.114	30.218	14
9095.09	Ca I]		9095.94	0.073	0.021	15
9123.60	[Cl II]	1F	9124.42	0.062	0.018	15
9204.17	O II		9204.98	0.044	0.013	16
9210.28	He I	6/9	9210.79	0.289	0.081	14
9213.20	He I	7/9	9213.54	0.044	0.012	17
9218.47	Fe I]		9219.10	0.032	0.009	18
9229.01	H I	P9	9229.49	7.093	1.989	14
9463.57	He I	1/5	9464.04	0.336	0.091	15
9516.57	He I	4/7	9517.18	0.110	0.030	15
9526.16	He I	6/8	9526.66	0.192	0.051	15
9530.60	[S III]	1F	9531.48	271.299	72.548	15
9535.41	O II		9536.05	0.071	0.019	16
9545.97	H I	P8	9546.51	9.377	2.502	15
9702.44	Cl I ?		9702.66	0.102	0.027	16
9824.13	[C I]	1F	9825.03	0.061	0.016	16
9834.7	O II		9835.46	0.043	0.011	17
9850.24	[C I]	1F	9851.10	0.269	0.071	15
9903.46	C II	17.02	9904.00	0.205	0.052	16
9962.63	O II	105.06	9963.05	0.022	0.005	:
10005.4	S II		10005.98	0.047	0.012	17
10008.6	Ne I		10009.21	0.032	0.008	19
10027.7	He I	6/7	10028.23	0.784	0.194	16
10031.2	He I	7/7	10031.65	0.252	0.062	16
10049.4	H I	P7	10049.91	20.915	5.175	16
10138.4	He I	10/7	10138.89	0.112	0.027	16
10286.7	[S II]	3F	10287.46	1.190	0.288	16
10310.7	He I	4/6	10311.82	0.538	0.130	16
10320.5	[S II]	3F	10321.24	1.459	0.353	16
10336.4	[S II]	3F	10337.17	1.057	0.255	16
10344.7	N I		10345.23	0.271	0.065	16
10344.8	N I					

^a Blend with sky emission line.

intensity ratios, all of them were re-scaled to $H\beta$. In the case of the bluest spectra (3000–3900 Å and 3800–5000 Å) all the intensity ratios, formerly referred to H9, were multiplied by the H9/ $H\beta$ ratio obtained in the short exposure spectrum of the 3800–5000 Å range. The emission line ratios of the 4750–6800 Å range were re-scaled to $H\beta$ multiplying by the $\text{He I } \lambda 5876 \text{ \AA}/H\beta$ ratio obtained from the shorter exposure spectrum. In the case of the last spectral section,

6700–10400 Å, the [S II] λ 6731 Å/H β ratio obtained for the 4750–6800 Å spectrum was the re-scaling factor used.

The different four spectral ranges covered in the spectra have overlapping regions at the edges. The final intensity of a given line in the overlapping regions is the average of the values obtained in both spectra. The differences in the intensity measured for each line in overlapping spectra do not show systematic trends and are always of the order or smaller than the quoted line intensity uncertainties. The final list of observed wavelengths, identifications and line intensities relative to H β is presented in Table 2.

For a given line, the observed wavelength is determined by the centre of the baseline chosen for the flux integration procedure or the centroid of the line when a Gaussian fit is used (in the case of line-blending). For the lines measured in the overlapping spectral regions, the average of the two independent determinations has been adopted. The final values of the observed wavelengths are relative to the heliocentric reference frame.

The identification and adopted laboratory wavelengths of the lines collected in Table 2 were obtained following previous identifications in the Orion nebula by EPTE and Baldwin et al. (1991), the identifications for 30 Dor by Peimbert (2003) and the compilations of Moore (1945, 1993), Wiese, Smith & Glennon (1966) and The Atomic Line List v2.04². This last interactive source of nebular line emission data was used directly or through the EMILI³ code (Sharpee et al. 2003). A large number of sky emission lines were identified –specially in the red part of the spectrum– but are not included in Table 2. About 11 emission lines could not be identified in any of the available references. Other 34 lines show a rather dubious identification. In total, about 8% of the lines are not identified or their identifications are not confident. The four unidentified lines reported in Table 3 of EPTE have been observed again and identified as faint C II or O II lines.

The reddening coefficient, $C(H\beta)$, was determined by fitting iteratively the observed Balmer decrement to the theoretical one computed by Storey & Hummer (1995) for the nebular conditions determined in Section 4. Following EPTE we have used the reddening function, $f(\lambda)$, normalized at H β derived by Costero & Peimbert (1970) for the Orion nebula. A linear extrapolation of this reddening function was used for wavelengths between 3000–3500 Å. To obtain the final value of $C(H\beta)$ we have taken the average of the values obtained from the intensity ratios of 21 Balmer and Paschen lines with respect to H β –from H10 to P7– with the exception of those H I lines showing line blending. The final adopted value of $C(H\beta)$ is 0.76 ± 0.08 , which is larger than the values of 0.39 ± 0.04 and 0.60 reported by EPTE and Peimbert & Torres-Peimbert (1977) for the same zone of the nebula. Table 2 shows the reddening-corrected line intensity ratios, $I(\lambda)/I(H\beta)$, for each line. The integrated reddening-corrected H β line flux is 9.32×10^{-11} erg cm⁻² s⁻¹.

In the case of the Orion nebula, there are several previous works presenting large lists of observed emission lines (Kaler, Aller & Bowen 1965; Osterbrock et al. 1992; EPTE; Baldwin et al. 2000). EPTE show a comparison be-

tween their datasets and those of Kaler et al. (1965) and Osterbrock et al. (1992), finding a good consistency with the second but detecting systematic differences with the older photographic data by Kaler et al. (1965). We have compared our VLT line intensity ratios with those of the two most recent previous spectroscopic works: EPTE and Baldwin et al. (2000). In Figure 1 we compare the reddening-corrected emission line ratios obtained in previous works and in our spectra for the lines in common by means of least-squares fits. The comparison with the data of EPTE shows a slope of 0.987, indicating a rather good consistency between both datasets. It must be taken into account that both observations correspond to the same zone of the nebula, although the integrated area is not exactly the same. On the other hand, the comparison with the data of Baldwin et al. (2000) gives a slope of 1.027, also fairly good, although there is an apparent trend of a slight overestimation of the intensity of the brightest lines (those with $\log[I(\lambda)/I(H\beta)] \geq -2.5$) in the dataset of Baldwin et al. (2000) with respect to ours. The slit position observed by Baldwin et al. (2000) does not coincide with our position, although it can be considered rather close taking into account the large angular size of the Orion nebula. Their position is located 25 arcsec north and 17 arcsec west of the centre of our slit position. We have also detected that the intensity ratios of the emission lines blueward of about 5000 Å tend to be higher in Baldwin et al. (2000) with respect to the data of both EPTE and ours. This trend is not observed when the datasets of EPTE and ours are compared.

In Figure 2, we show part of our flux calibrated echelle spectrum around the lines of multiplet 1 of O II. The same spectral range is presented by EPTE and Baldwin et al. (2000). Readers can compare the signal-to-noise ratio and the spectral resolution of each of the three sets of echelle spectra.

The observational errors associated with the line intensities (in percentage of their ratio with respect H β) are also presented in Table 2. These errors include the uncertainties in the line intensity measurement and flux calibration as well as the propagation of the uncertainty in the reddening coefficient. Colons indicate errors of the order of or larger than 40%.

4 PHYSICAL CONDITIONS

The electron density, N_e , has been derived from the ratio of collisionally excited lines of several ions and making use of NEBULAR routines (Shaw & Dufour 1995) included in the IRAF package. In the case of [Fe III], we have obtained the value of N_e that minimizes the dispersion of the line ratios of 14 individual [Fe III] emission lines with respect to [Fe III] λ 4658 Å. The calculations for this ion have been done with a 34 level model-atom that uses the collision strengths of Zhang (1996) and the transition probabilities of Quinet (1996). The [O II] electron density has been obtained from two different line ratios $I(3729)/I(3726)$ and $I(3726 + 3729)/I(7319 + 7320 + 7331 + 7332)$. The contribution of the intensities of the [O II] $\lambda\lambda$ 7319, 7320, 7331, and 7332 lines due to recombination has been taken into account following the expression given by Liu et al. (2000). In

² webpage at: <http://www.pa.uky.edu/~peter/atomic/>

³ webpage at: <http://www.pa.msu.edu/astro/software/emili/>

Table 3. Physical conditions.

Parameter	Line	Value
N_e (cm ⁻³)	[N I]	1700±600
	[O II] ^a	2400±300
	[O II] ^b	6650±400
	[S II]	6500 ⁺²⁰⁰⁰ ₋₁₂₀₀
	[Fe III]	9800±300
	[Cl III]	9400 ⁺¹²⁰⁰ ₋₇₀₀
	[Ar IV]	6800 ⁺¹¹⁰⁰ ₋₁₀₀₀
T_e (K)	[O I]	8000:
	[C I]	>10000
	[N II]	10150±350
	[O II]	9800±800
	[S II]	9050±800
	[O III]	8300±40
	[S III]	10400 ⁺⁸⁰⁰ ₋₁₂₀₀
	[Ar III]	8300±400
	Bac	7900±600
	Pac	8100±1400

^a From 3726/3729 ratio.

^b From (3727+9)/(7319+20+31+32) ratio.

any case, this contribution is rather small (about 3% of the total intensity).

From Table 3, one can see that the density obtained from the [O II] $I(3729)/I(3726)$ line ratio is lower than the values obtained from most of the other indicators. This effect is also reported in other objects recently studied by our group: NGC 3576 (García-Rojas et al. 2004) and NGC 5315 (Peimbert et al. 2004) as well as marginally in low-density H II regions as 30 Dor (Peimbert 2003) and NGC 2467 (García-Rojas et al., in preparation), where $N_e(\text{O II})$ is somewhat lower than the densities derived from the other density indicators. Moreover, in the case of our data for the Orion nebula, adopting the density derived from [O II] $I(3729)/I(3726)$, we find: a) the electron temperature for O^+ – $T_e(\text{O II})$ – is higher than the rest of ionic temperatures; b) a larger dispersion in the ionic abundances obtained from the individual [O II] lines. Alternatively, we have derived the electron density from the [O II] $I(3726 + 3729)/I(7319 + 7320 + 7331 + 7332)$ line ratio, finding that: a) the density is now more consistent with the rest of the indicators; b) the dispersion of the O^+/H^+ ratios obtained from the different individual lines is lower. Therefore, it seems more advisable to rely in the $N_e(\text{O II})$ obtained from the [O II] $I(3726 + 3729)/I(7319 + 7320 + 7331 + 7332)$ ratio. We find that this indicator is also more consistent in the cases of NGC 3576, NGC 5315 and NGC 2467. For comparison, we have determined $N_e(\text{O II})$ from $I(3729)/I(3726)$ line ratio making use of the old FIVEL program described by De Robertis, Dufour & Hunt (1987) –the program in which NEBULAR is based– finding that the value obtained is higher (4800 cm⁻³ instead of 2400 cm⁻³) becoming more similar to those obtained from the other density indicators. We also obtain systematically higher –and more consistent– values of $N_e(\text{O II})$ using FIVEL for NGC 3576, NGC 5315, NGC 2467 and 30 Dor. The structure of both programs –FIVEL and NEBULAR– is basically the same. Apparently, the only substantial difference is the atomic data used. NEBULAR is periodically updated and our version of

FIVEL is not updated since 1996. In the case of O II, FIVEL uses the transition probabilities of Zeippen (1982) and collision strengths of Pradhan (1976) and the last version of NEBULAR uses the transition probabilities recommended by Wiese, Fuhr & Deters (1996) and the collision strengths of McLaughlin & Bell (1993). We think that the problem with the density derived from [O II] $I(3729)/I(3726)$ ratio could be due to errors or problems in the atomic data used for those transitions in the latest version of NEBULAR.

From Table 3, it seems that there are no apparent differences between densities for low and high-ionization-potential ions. Therefore, a value of 8900±200 cm⁻³ has been adopted as representative of our observed zone and all ions. This is a weighted average of the densities obtained from the [O II] $I(3726 + 3729)/I(7319 + 7320 + 7331 + 7332)$, [S II], [Fe III], [Cl III], and [Ar IV] emission line ratios. This value is somewhat larger than the electron density of 5700 cm⁻³ adopted by EPTE.

As in the case of densities, electron temperatures, T_e , have been derived from the ratio of collisionally excited emission lines of several ions and making use of NEBULAR routines. In the case of the [N II] λ 5755 Å line, we have corrected its intensity for the contribution of recombination following Liu et al. (2000). This contribution is very small, about 2%.

The echelle spectra show enough good signal-to-noise ratio for the nebular continuum emission to allow a satisfactory determination of both the Balmer and Paschen discontinuities (see Figure 3). They are defined as $I_c(\text{Bac}) = I_c(\lambda 3646^-) - I_c(\lambda 3646^+)$ and $I_c(\text{Pac}) = I_c(\lambda 8203^-) - I_c(\lambda 8203^+)$ respectively. The high spectral resolution of the spectra permits to measure the continuum emission in zones very near de discontinuity, minimizing the possible contamination of other continuum contributions. We have obtained power-law fits to the relation between $I_c(\text{Bac})/I(Hn)$ or $I_c(\text{Pac})/I(Pn)$ and T_e for different n corresponding to different observed lines of both series. The emissivities as a function of electron temperature for the nebular continuum and the H I Balmer and Paschen lines have been taken from Brown & Mathews (1970) and Storey & Hummer (1995) respectively. The $T_e(\text{Bac})$ adopted is the average of the values using the lines from $H\alpha$ to H 10 (the brightest ones). In the case of $T_e(\text{Pac})$, the adopted value is the average of the individual temperatures obtained using the lines from P 7 to P 18 (the brightest lines of the series), excluding P 8 and P 10 because their intensity seems to be affected by sky absorption. As it can be seen in Table 3, $T_e(\text{Bac})$ and $T_e(\text{Pac})$ are remarkably similar despite their relatively large uncertainties.

We have adopted the average of electron temperatures obtained from [N II], [S II], and [O II] lines as representative for the low ionization zone, $T_{low} = 10000\pm 400$ K, and the average of the values obtained from [O III], [S III], and [Ar III] lines for the high ionization zone, $T_{high} = 8320\pm 40$ K. The temperatures adopted by EPTE were $T_{low} = 10710\pm 450$ K and $T_{high} = 8350\pm 200$ K.

5 HE⁺ ABUNDANCE

We have observed a large number of He I lines in our spectra. These lines arise mainly from recombination

Table 4. He⁺ abundance.

Line	He ⁺ /H ⁺ ^a
3819.61	911 ± 27
3888.65	860 ± 26
3964.73	868 ± 26
4026.21	914 ± 27
4387.93	861 ± 17
4471.09	852 ± 9
4713.14	884 ± 9
4921.93	886 ± 9
5875.64	907 ± 27
6678.15	912 ± 55
7065.28	626 ± 44
7281.35	738 ± 59
Adopted	874 ± 6 ^b

^a In units of 10⁻⁴, for $\tau_{3889} = 16.7 \pm 0.5$ and $t^2 = 0.022 \pm 0.002$. Uncertainties correspond to line intensity errors.

^b It includes all the relevant uncertainties in emission line intensities, N_e , τ_{3889} and t^2 .

but they can be affected by collisional excitation and self-absorption effects. We have determined the He⁺/H⁺ ratio using the effective recombination coefficients of Storey & Hummer (1995) for H I, and those by Smits (1996) and Benjamin, Skillman & Smits (1999) for He I. The collisional contribution was estimated from Sawey & Berrington (1993) and Kingdon & Ferland (1995), and the optical depth effects in the triplet lines were estimated from the computations by Benjamin, Skillman & Smits (2002). From a maximum likelihood method (e. g. Peimbert, Peimbert & Ruiz. 2000), using $N_e = 8900 \pm 200 \text{ cm}^{-3}$ and $T(\text{O II+III}) = 8730 \pm 320 \text{ K}$ (see Sect. 8), we obtained $\text{He}^+/\text{H}^+ = 0.0874 \pm 0.0006$, $\tau_{3889} = 16.7 \pm 0.5$, and $t^2 = 0.022 \pm 0.002$. In Table 4 we include the He⁺/H⁺ ratios we obtain for the best observed individual He I lines (those lines not affected by line blending and with the highest S/N for which we expect to have the best atomic data, i.e. low n upper level) as well as the final adopted value, all the values are computed for our finally adopted $t^2 = 0.022 \pm 0.002$ (see Sect. 8). We have also excluded He I 5015 Å because it could suffer self-absorption effects from the 2¹S metastable level. If we make a simple χ^2 optimisation of the values given in the table, we obtain a χ^2 parameter of about 45, which indicates that the goodness of fit is rather poor. The value of $\tau_{3889} = 16.7$ we obtain is very large and therefore the self-absorption corrections for triplets are large and perhaps rather uncertain. Moreover, the slit position observed is very near the Trapezium stars and underlying absorption by the dust-scattered stellar continua can be affecting the intensity of the He I lines. Therefore, the adopted He⁺ abundance can be affected by additional systematic uncertainties very difficult to estimate.

6 IONIC ABUNDANCES FROM COLLISIONALLY EXCITED LINES

Ionic abundances of N⁺, O⁺, O⁺⁺, Ne⁺⁺, S⁺, S⁺⁺, Cl⁺⁺, Cl³⁺, Ar⁺⁺, and Ar³⁺ have been obtained from collisionally excited lines (CELs) using the NEBULAR routines of the IRAF package. We have assumed a two-zone scheme and $t^2=0$, adopting the values of $T_{low} = 10000 \pm 400 \text{ K}$ for low-

Table 5. Ionic abundances from collisionally excited lines^a.

Ion	$t^2=0.000$	$t^2=0.022 \pm 0.002$
He ⁺	10.940 ± 0.003	10.937 ± 0.003
N ⁺	6.90 ± 0.09	6.96 ± 0.09
O ⁺	7.76 ± 0.15	7.90 ± 0.15
O ⁺⁺	8.43 ± 0.01	8.59 ± 0.03
Ne ⁺⁺	7.69 ± 0.07	7.86 ± 0.07
S ⁺	5.40 ± 0.06	5.47 ± 0.06
S ⁺⁺	7.01 ± 0.04	7.18 ± 0.05
Cl ⁺	4.84 ± 0.11	4.90 ± 0.11
Cl ⁺⁺	5.14 ± 0.02	5.30 ± 0.02
Cl ³⁺	3.79 ± 0.12	3.92 ± 0.12
Ar ⁺⁺	6.37 ± 0.05	6.50 ± 0.05
Ar ³⁺	4.60 ± 0.03	4.76 ± 0.04
Fe ⁺⁺	5.37 ± 0.08	5.53 ± 0.08
Fe ³⁺	5.65 ^{+0.19} _{-0.30}	5.78 ^{+0.19} _{-0.30}

^a In units of $12 + \log(X^m/\text{H}^+)$.

ionization-potential ions (N⁺, O⁺, S⁺, and Cl⁺) and $T_{high} = 8320 \pm 40 \text{ K}$ for the high-ionization-potential ions (O⁺⁺, Ne⁺⁺, S⁺⁺, Cl⁺⁺, Cl³⁺, Ar⁺⁺, and Ar³⁺). The density assumed is the same for all ions, $N_e = 8900 \pm 200$. The ionic abundances are listed in Table 5. Many [Fe II] lines have been identified in our spectra but all of them are affected by fluorescence effects (Rodríguez 1999; Verner et al. 2000). Unfortunately, we can not measure the [Fe II] $\lambda 8617 \text{ \AA}$ line, which is almost insensitive to the effects of UV pumping. This line is precisely in one of the observational gaps of our spectroscopic configuration. Therefore, it was not possible to derive a confident value of the Fe⁺/H⁺ ratio. The Fe⁺⁺/H⁺ ratio has been derived from the average of the values obtained from 14 individual emission lines. The calculations for this ion have been done with a 34 level model-atom that uses the collision strengths of Zhang (1996) and the transition probabilities of Quinet (1996). In the case of Fe³⁺/H⁺ ratios, we have used a 33-level model-atom where all collision strengths are those calculated by Zhang & Pradhan (1997), the transition probabilities are those recommended by Froese Fischer & Rubin (1998) (and those from Garstang 1998 for the transitions not considered by Froese Fischer & Rubin). The Cl⁺/H⁺ ratio cannot be derived from the NEBULAR routines, instead we have used an old version of the five-level atom program of Shaw & Dufour (1995) –FIVEL– that is described by De Robertis et al. (1987). This program uses the atomic data for Cl⁺ compiled by Mendoza (1983). In any case, the atomic data for this ion –and therefore the Cl⁺/H⁺ ratio– are rather uncertain (Shaw 2003, personal communication).

7 IONIC ABUNDANCES OF HEAVY ELEMENTS FROM RECOMBINATION LINES

The large sensitivity and spectral coverage of these new observations have increased dramatically the number of permitted lines measured in this particular zone of the Orion nebula with respect to the previous results of EPTE. We have detected lines of: C II, N I, N II, N III, O I, O II, O III, Ne I, Ne II, Ne III, Si I, Si II, Si III, S II, S III, and perhaps

some possible lines of Mg I, Al II, Ar II, Cr II, Mn II, Fe I, Fe II, and Ni II.

The excitation mechanisms of many permitted lines observed in the Orion nebula have been discussed by Grandi (1975a, b; 1976) and EPTE. Most of these lines are produced by continuum and/or line fluorescence but some of them by recombination. Recombination lines are the only ones useful for abundance determinations. We have derived the ionic abundances for those ions with effective recombination coefficients available in the literature. EPTE only derive the C^{++}/H^+ and O^{++}/H^+ ratios from their data but we can now also obtain values for O^+/H^+ , N^{++}/H^+ , and Ne^{++}/H^+ from recombination lines. We have also derived the abundances from N I lines, but they are found to be useless because they are largely produced by starlight excitation. The ionic abundances obtained from permitted lines of heavy elements are shown in Tables 6 to 11. We have derived the abundance of the whole multiplet in the case of those multiplets with more than two lines observed ("Sum" in the tables). To derive the sum value we have used the effective recombination coefficient of the multiplet and the expected intensity of the whole multiplet. This last quantity has been obtained adding the intensity of the observed lines multiplied by the quotient of the gf value of the whole multiplet with respect to the sum of the gf values of the observed individual lines. EPTE describe the method with more detail. We prefer the sum value because it provides a weighted average of the abundances derived from each line of the multiplet and it washes out possible departures from the LTE predictions inside the multiplet. We have adopted T_{high} for C^{++} , O^{++} , N^{++} , and Ne^{++} ; T_{low} for O^+ and N^+ .

We have effective recombination coefficients for multiplets 2, 3, 6, 16.04, 17.02, 17.04 and 17.06 of C II (Davey, Storey, & Kisielius 2000). The C^{++}/H^+ ratios obtained are shown in Table 6. The upper level of multiplet 3 can be populated by resonance fluorescence by starlight from the ground state and this can explain its corresponding abnormally large C^{++}/H^+ ratio. Resonance fluorescence by starlight can be also operating on multiplet 2 (EPTE). The rest of the multiplets included in Table 6 are produced by transitions involving levels with large l quantum numbers and cannot be excited by permitted resonance transitions from the ground level. Therefore, their excitation mechanism should be recombination and their C^{++}/H^+ ratios should reflect the true abundance of that ion. The C^{++}/H^+ ratios obtained from the different C II lines coming from large l levels show an excellent agreement. These values are also case-independent. The final adopted C^{++}/H^+ ratio is $(22\pm 1)\times 10^{-5}$. This value has been obtained from the weighted mean of the individual abundances obtained from multiplets 6, 16.04, 17.02, 17.04, and 17.06. In Figure 4 we show some of these pure recombination C II lines used to derive the final C^{++} abundance. EPTE obtained a $C^{++}/H^+=20\times 10^{-5}$ for the same zone using the older effective recombination coefficients by Péquignot, Petitjean & Boisson (1991). All the individual abundance values used to derive the adopted average are indicated in boldface in Table 6.

Grandi (1975a) showed that the upper levels of the transitions of multiplets 1, 2, and 3 of N I should be significantly populated by starlight excitation. In Table 7, we show the N^+/H^+ ratios we obtain using the effective re-

combination coefficients of Péquignot et al. (1991). The abnormally large abundances obtained indicate that starlight excitation is the dominant mechanism of those multiplets, therefore the abundances derived from the observed N I are –unfortunately– useless for our purposes and will not be considered.

We have measured a large number of N II lines in our spectra. Grandi (1976) showed that multiplets 3 and 5 of N II in the Orion nebula may be excited by resonance fluorescence via the He I λ 508.6 Å line. Tsamis et al. (2003) also suggest that N II triplet lines of the spectra of their sample H II regions can be affected by fluorescence. The ground state of N II is a triplet and, therefore, singlet lines are expected to be produced by pure recombination and should not be affected by fluorescence effects. We have only poor detections of three very weak singlet lines, which are not confident for abundance determinations. Moreover, the brightest singlet line reported could be a misidentification. There are three different sets of effective recombination coefficients available for N II (Escalante & Victor 1990; Péquignot et al. 1991; Kisielius & Storey 2002), the N^{++}/H^+ ratios obtained for all the lines and sets of coefficients are shown in Table 8. We have adopted case B as representative for triplets and obtained quite similar values of the N^{++}/H^+ ratio for all the triplet multiplets observed. We have obtained a weighted mean of the abundance considering multiplets 3, 4, 5, 11 and 22 (sum values of the multiplet when more than two lines of the multiplet are reported) and the effective recombination coefficients of Escalante & Victor (1990) and multiplets 3, 12, 24 and 28 and the coefficients of Péquignot et al. (1991), finding the same value in both cases: $N^{++}/H^+=12\times 10^{-5}$. This value is somewhat lower than the final adopted abundance using the most recent effective recombination coefficients by Kisielius & Storey (2002) and the weighted mean of the N^{++}/H^+ ratios obtained using multiplets 3, 4, 5, 19, 20, 24 and 28. In fact, from Table 8, it is clear that the individual values of the abundance obtained using Kisielius & Storey (2002) are always somewhat larger than those obtained with the other two sources of effective recombination coefficients. All the individual abundance values used to derive the adopted average are indicated in boldface in Table 8. This final N^{++}/H^+ ratio gives a total N abundance which is abnormally high (see Sect. 9) independently of the recombination coefficients set used, indicating that the lines used in Table 8 for deriving the abundance are not produced by pure recombination and, unfortunately, not suitable for abundance determinations. This result has been also obtained by Tsamis et al. (2003).

Several O I lines are identified and measured in our spectra. Most of them correspond to transitions between triplet levels that can be excited from the ground state ($2p^4\ ^3P$) by starlight excitation, as it was demonstrated by Grandi (1975b). We have measured lines of multiplet 1 of O I, which corresponds to transition between quintet levels. In principle, these lines should be produced by pure recombination and are also case-insensitive. Lines of multiplet 1 of O I are in a spectral region with numerous sky emission lines. Unfortunately, the combination of our spectral resolution and the radial velocity of Orion nebula does not permit to deblend the brightest line of multiplet 1 at λ 7771.94 Å and an underlying sky emission feature. Therefore, we have to rely on the O^+/H^+ ratio obtained from the faint O I λ 7775.34

Table 6. C⁺⁺/H⁺ ratios from Permitted Lines

Mult.	Transition	λ_0	$I(\lambda)/I(H\beta)$ ($\times 10^{-2}$)	C ⁺⁺ /H ⁺ ($\times 10^{-5}$) ^a	
				A	B
2	3s ² S–3p ² P ⁰	6578.05	0.29±0.02	330±20	56±3
3	3p ² P ⁰ –3d ² D	7231.34	0.073±0.007	1900±200	2700±300
		7236.42	0.24±0.02	3700±700	5200±400
		Sum	0.54±0.04	3700±300	4300±300
6	3d ² D–4f ² F ⁰	4267.26	0.24±0.01	22±1	–
16.04	4d ² D–6f ² F ⁰	6151.43	0.009±0.003	20±7	–
17.02	4f ² F ⁰ –5g ² G	9903.46	0.052±0.008	19±3	–
17.04	4f ² F ⁰ –6g ² G	6461.95	0.025±0.004	21±3	–
17.06	4f ² F ⁰ –7g ² G	5342.40	0.013±0.004	23±7	–
Adopted				22±1	

^a Effective recombination coefficients by Davey et al. (2000).

Table 7. N⁺/H⁺ ratios from Permitted Lines

Mult.	Transition	λ_0	$I(\lambda)/I(H\beta)$ ($\times 10^{-2}$)	N ⁺ /H ⁺ ($\times 10^{-5}$) ^a	
				A	B
1	3s ⁴ P–3p ⁴ D ⁰	8680.28	0.033±0.005	95±13	92±13
		8683.40	0.029±0.004	160±20	150±20
		8686.15	0.025±0.004	350±50	340±50
		8703.25	0.021±0.003	270±40	260±40
		8711.70	0.022±0.003	240±40	230±40
		8718.83	0.013±0.002	180±30	180±30
		Sum	0.15±0.02	170±20	160±20
2	3s ⁴ P–3p ⁴ P ⁰	8210.72	0.003±0.001	120±40	110±40
		8216.34	0.026±0.003	160±20	140±20
		8223.14	0.053±0.006	780±90	670±80
		Sum	0.15±0.02	330±40	280±30
3	3s ⁴ P–3p ⁴ S ⁰	7423.64	0.012±0.002	1200±200	390±60
		7442.30	0.031±0.003	1500±200	490±50
		7468.31	0.044±0.004	1400±100	460±50
		Sum	0.09±0.01	1400±200	460±50

^a Effective recombination coefficients by Péquignot et al. (1991).

Å line, which has a large uncertainty. In any case, this is the first time the O⁺ abundance is derived from RLs in the Orion nebula. We have two sets of effective recombination coefficients available for O I in the literature, those by Escalante & Victor (1992) and Péquignot et al. (1991), both sets give quite similar values of the abundances. In Table 9, we show the O⁺/H⁺ ratios obtained for the different useful lines and multiplets. The values obtained from triplet lines are always much larger than those obtained from multiplet 1, demonstrating the important contribution of starlight excitation to the intensity of the triplet lines.

We have identified and measured a large number of O II lines in our spectra. The largest collection of this kind of lines ever identified in an H II region. In our inventory, there are lines coming from transitions between both possible kinds of levels: doublets and quartets. Grandi (1976) demonstrated the dominance of recombination in the excitation mechanism of the O II spectrum. We have also measured several lines coming from 4f–3d transitions and these lines cannot be excited by fluorescence from the 2p³ 4S⁰ ground level. We have used effective recombination coefficients from Storey (1994) for 3s–3p and 3p–3d transitions (assuming LS-coupling), and from Liu et al. (1995) for 3p–3d and 3d–4f transitions (assuming intermediate cou-

pling). We used the dielectronic recombination coefficients of Nussbaumer & Storey (1984) for multiplets 15, 16 and 36. The final adopted value of the O⁺⁺/H⁺ ratio has been obtained from the weighted mean of the sum values of those less case-dependent multiplets: number 1, 2 and 10 and all the 4f–3d transitions. Our O⁺⁺ abundance coincides with that obtained by EPTE for the same zone of the Orion nebula. All the individual abundance values used to derive the adopted average are indicated in boldface in Table 10.

Several Ne II lines are identified and measured in the blue spectral range covered with our data. These lines correspond to doublet, quartet and intercombination transitions. We have used the effective recombination coefficients computed by Kisielius et al. (1998) for deriving the Ne⁺⁺/H⁺ ratios shown in Table 11. We have used the quartet Ne II lines to obtain the final adopted Ne⁺⁺ abundance (the weighed average of the values obtained from the individual lines). These lines are case-independent and are very probably produced by pure recombination because the ground level has doublet configuration. In Figure 5 we show some of the quartet lines used to derive the Ne⁺⁺ abundance. This is the first time the Ne⁺⁺/H⁺ ratio is derived from recombination lines in the Orion nebula.

Table 8. N⁺⁺/H⁺ ratios from Permitted Lines

Mult.	Transition	λ_0	$I(\lambda)/I(H\beta)$ ($\times 10^{-2}$)	N ⁺⁺ /H ⁺ ($\times 10^{-5}$)					
				E&V90 ^a		PPB91 ^b		K&S02 ^c	
				A	B	A	B	A	B
1	2p ³ 1D ⁰ –3p ¹ P	4895.11	0.015±0.004	36±9	–	–	–	–	–
3	3s ³ P ⁰ –3p ³ D	5666.64	0.029±0.004	9±1	8±1	12±2	10±2	16±2	13±2
		5676.02	0.010:	7:	6:	9:	8:	13:	10:
		5679.56	0.043±0.004	7±1	6±1	10±1	8±1	13±1	11±1
		5686.21	0.006:	6:	5:	8:	6:	10:	8:
		5710.70	0.009±0.003	9±3	8±3	11±4	9±3	15±5	13±4
		Sum	0.112±0.009	8±1	7±1	10±1	8±1	14±1	11±1
4	3s ³ P ⁰ –3p ³ S	5045.10	0.014±0.003	70±20	12±2	–	–	170±40	23±5
5	3s ³ P ⁰ –3p ³ P	4601.48	0.013±0.004	60±20	11±3	–	–	100±30	17±5
		4613.87	0.010±0.003	100±30	19±6	–	–	170±60	30±7
		4621.39	0.016±0.004	110±30	20±5	–	–	180±40	32±3
		4630.54	0.048±0.005	70±7	13±1	–	–	110±10	20±2
		4643.06	0.015±0.004	65±10	12±2	–	–	110±20	19±3
		Sum	0.115±0.006	73±4	14±1	–	–	120±6	21±1
12	3s ¹ P ⁰ –3p ¹ D	3994.99	0.010:	13:	12:	–	–	11:	11:
19	3p ³ D–3d ³ F ⁰	5001.47	0.030±0.005	–	–	9±1	9±1	7±1	7±1
20	3p ³ D–3d ³ D ⁰	4803.29	0.019±0.004	9±2	9±2	–	–	12±2	24±4
		4779.71	0.011±0.003	14±4	14±4	–	–	19±6	40±10
		4788.13	0.014±0.004	12±3	11±3	–	–	16±4	31±8
		Sum	0.056±0.006	11±1	11±1	–	–	15±2	28±3
		4994.37	0.018±0.006	23±8	22±8	–	18±6	700±200	30±10
28	3p ³ P–3d ³ D ⁰	5927.82	0.010:	–	–	–	25:	1800:	35:
		5931.78	0.020±0.004	–	–	–	21±4	1600±300	30±6
		5941.65	0.015±0.004	–	–	–	9±2	600±200	12±3
		5952.39	0.012:	–	–	–	39:	2800:	55:
		Sum	0.063±0.005	–	–	–	17±1	1200±100	24±2
29	3p ¹ S–5d ¹ P ⁰	5495.70	0.005:	–	–	–	4:	–	–
39	3d ³ F ⁰ –4f ⁷ [3 $\frac{1}{2}$]	4041.31	0.013:	–	–	–	3:	–	–
Adopted								20±1	

^a Effective recombination coefficients by Escalante & Victor (1990).

^b Effective recombination coefficients by Péquignot et al. (1991).

^c Effective recombination coefficients by Kisielius & Storey (2002).

Table 9. O⁺/H⁺ ratios from Permitted Lines

Mult.	Transition	λ_0	$I(\lambda)/I(H\beta)$ ($\times 10^{-2}$)	O ⁺ /H ⁺ ($\times 10^{-5}$)			
				E&V92 ^a		PPB91 ^b	
				A	B	A	B
1	3s ⁵ S ⁰ –3p ⁵ P	7771.94	0.016 ^c	21:	–	16:	–
		7775.34	0.006±0.001	16±3	–	12±2	–
4	3s ³ S ⁰ –3p ³ P	8446.48	0.9±0.1	5100±600	1000±100	3300±400	760±90
5	3s ³ S ⁰ –4p ³ P	4368.19	0.073±0.007	880±80	180±20	–	–
10	3p ⁵ P–4d ⁵ D ⁰	6155.98	0.005:	71:	70:	–	–
20	3p ³ P–5s ³ S ⁰	7254.40	0.11±0.01	7300±600	2300±200	–	–
21	3p ³ P–4d ³ D ⁰	7002.10	0.086±0.007	420±30	390±30	–	–
22	3p ³ P–6s ³ S ⁰	6046.40	0.089±0.006	11500±800	5200±400	–	–
23	3p ³ P–5d ³ D ⁰	5958.39	0.038±0.005	320±40	310±40	–	–
24	3p ³ P–7s ³ S ⁰	5554.83	0.025±0.004	–	3900±700	–	–
25	3p ³ P–6d ³ D ⁰	5512.77	0.024±0.004	340±60	330±60	–	–
26	3p ³ P–8s ³ S ⁰	5298.89	0.028±0.005	–	11000±2000	–	–
27	3p ³ P–7d ³ D ⁰	5274.97	0.011±0.003	–	250±80	–	–
Adopted						14±4	

^a Effective recombination coefficients by Escalante & Victor (1992).

^b Effective recombination coefficients by Péquignot et al. (1991).

^c Blend with sky emission line.

Table 10. –continued

Mult.	Transition	λ_0	$I(\lambda)/I(H\beta)$ ($\times 10^{-2}$)	O^{++}/H^+ ($\times 10^{-5}$)							
				S94 ^a			LSBC95 ^b			NS84 ^c	
				A	B	C	A	B	C	–	
3d-4f	3d ⁴ F–4fG ² [4] ⁰	4083.90	0.010±0.004	–	–	–	30±10	–	–	–	
	3d ⁴ F–4fG ² [3] ⁰	4087.15	0.013±0.004	–	–	–	40±10	–	–	–	
	3d ⁴ F–4fG ² [5] ⁰	4089.29	0.025±0.005	–	–	–	22±4	–	–	–	
	3d ⁴ F–4fG ² [3] ⁰	4095.64	0.007:	–	–	–	31:	–	–	–	
	3d ⁴ F–4fD ² [3] ⁰	4107.09	0.006:	–	–	–	46:	–	–	–	
	3d ⁴ F–4fF ² [4] ⁰	4062.94	0.006:	–	–	–	42:	–	–	–	
	3d ⁴ P–4fD ² [2] ⁰	4307.23	0.007:	–	–	–	58:	–	–	–	
	3d ⁴ D–4fG ² [4] ⁰	4332.69	0.020±0.004	–	–	–	180±40	–	–	–	
	3d ⁴ D–4fF ² [4] ⁰	4275.55	0.017±0.004	–	–	–	27±6	–	–	–	
	3d ² D–4fF ² [4] ⁰	4609.44	0.013±0.004	–	–	–	27±7	–	–	–	
	3d ² D–4fF ² [3] ⁰	4602.11	0.005:	–	–	–	26:	–	–	–	
		Sum		0.11±0.01	–	–	–	30±3	–	–	–
	Adopted							37±1			

^a Effective recombination coefficients by Storey (1994).

^b Effective recombination coefficients for intermediate coupling by Liu et al. (1995).

^c Dielectronic recombination rates by Nussbaumer & Storey (1984).

^d Expected total intensity of the multiplet assuming LS coupling.

^e Expected total intensity of the multiplet assuming intermediate coupling.

^f Expected total intensity of the multiplet assuming intermediate coupling and case A.

^g Expected total intensity of the multiplet assuming intermediate coupling and case B.

^h Expected total intensity of the multiplet assuming intermediate coupling and case C.

Table 11. Ne⁺⁺/H⁺ ratios from Permitted Lines

Mult.	Transition	λ_0	$I(\lambda)/I(H\beta)$ ($\times 10^{-2}$)	Ne ⁺⁺ /H ⁺ ($\times 10^{-5}$) ^a	
				A	B
1	3s ⁴ P–3p ⁴ P ⁰	3694.22	0.04±0.01	12±4	–
2	3s ⁴ P–3p ⁴ D ⁰	3334.87	0.09±0.02	14±3	–
7	3s ² P–3p ² P ⁰	3323.75	0.06±0.02	20±7	–
19	3p ² D ⁰ –3d ⁴ F	3388.46	0.03:	10:	9:
39	3p ² P ⁰ –3d ⁴ D	3829.77	0.02:	250:	15 :
57	3d ⁴ F–4f ⁴ G ⁰	4391.94	0.014±0.004	4±1	–
		4409.30	0.009±0.003	4±1	–
	Sum		0.023±0.005	4±1	–
Adopted				9±2	

^a Effective recombination coefficients by Kisielius et al. (1998).

8 IONIC ABUNDANCES FROM CELS AND RLS AND TEMPERATURE VARIATIONS

Ionic abundances derived from CELs and RLs are systematically different in many ionized nebulae (e. g. Liu 2002, 2003; Esteban 2002, Torres-Peimbert & Peimbert 2003). In fact, O⁺⁺/H⁺ ratios obtained from O II lines are between 0.1 to 0.3 dex larger than those obtained from [O III] lines in the few Galactic and extragalactic H II regions where both kinds of lines have been observed (EPTE; Esteban et al. 1999a, b, 2003; Peimbert 2003; Tsamis et al. 2003). A similar situation has been found in the case of C⁺⁺/H⁺ and O⁺/H⁺ ratios. In Table 12 we compare the different ionic abundances we have obtained from CELs and RLs of the same ions. The RLs abundances are the "Adopted" ones given in Tables 6 to 11. In the case of the C⁺⁺/H⁺ ratio obtained from CELs, we have taken the average of the values corresponding to slit positions 5 and 7 of Walter, Dufour & Hester (1992). As it

Table 12. Abundance discrepancies and t^2 parameter

	12+log(X ^m /H ⁺)		t^2
	CELS	RLs	
O ⁺	7.76±0.15	8.15±0.13	0.052±0.029
O ⁺⁺	8.43±0.01	8.57±0.01	0.020±0.002
C ⁺⁺	7.94±0.15 ^a	8.34±0.02	0.039±0.011
Ne ⁺⁺	7.69±0.07	7.95±0.07	0.032±0.014
He ⁺	0.022±0.002
T(Bac)/T(OII+OIII)	0.018±0.018
T(Pac)/T(OII+OIII)	0.013 ^{+0.033} _{-0.013}
Adopted	0.022±0.002

^a Abundance taken from Walter et al. (1992)

can be seen in Table 12, all the ionic abundances obtained from RLs are larger than the values derived from CELs.

Torres-Peimbert, Peimbert & Daltabuit (1980) proposed that the abundance discrepancy between calculations based on CELs and RLs may be produced by the presence of spatial fluctuations of the electron temperature in the nebulae, parametrized by t^2 (Peimbert 1967). Assuming the validity of the temperature fluctuations paradigm, the comparison of the abundances determined from both kinds of lines for a given ion should provide an estimation of t^2 . In Table 12 we include the t^2 values that produce the agreement between the abundance determinations obtained from CELs and RLs of O^+ , O^{++} , C^{++} and Ne^{++} . These calculations have been made following the formalism outlined by Peimbert & Costero (1969). As it can be seen in the table, the values of t^2 from the abundance discrepancies are—in general—fairly similar taking into account the uncertainties. In Table 12 we also include the t^2 value obtained from the application of the maximum-likelihood method to the He^+/H^+ ratios, obtained in Sect. 5. This value is in excellent agreement with that obtained for O^{++} . The comparison between electron temperatures obtained from intensity ratios of CELs and the Balmer or Paschen continua is an additional indicator of t^2 . However, since $T_e(\text{Bac})$ and $T_e(\text{Pac})$ are representative of the whole nebula, the T_e values obtained from CELs have to be considered only representative of the temperature of the zone where the ion producing the lines are located. Following Peimbert, Peimbert & Luridiana (2002) and Peimbert (2003), we have compared $T_e(\text{Bac})$ and $T_e(\text{Pac})$ with the combination of $T([\text{OII}])$ and $T([\text{OIII}])$ considering a weight, γ , between the OII and OIII zones given by:

$$\gamma = \frac{\int N_e N(O^{++}) dV}{\int N_e N(O^+) dV + \int N_e N(O^{++}) dV}. \quad (1)$$

Taking into account $\gamma \approx 0.83$ as representative for the center of the nebula (obtained from our derived abundances), we can obtain the average temperature $T(O \text{ II+III})$ using equation A1 of Peimbert et al. (2002), which gives: $T(O \text{ II+III}) = 8730 \pm 320$ K. In Table 12, we include the values of t^2 obtained from the combination of $T(O \text{ II+III})$ and $T(\text{Bac})$ and $T(\text{Pac})$. As we can see, the t^2 values obtained are rather consistent with the rest of determinations, especially with those obtained for O^{++} and He^+ , the ones with the lowest uncertainties. However, the nominal t^2 values derived from the Balmer and Paschen discontinuities should be considered lower limits to the real ones. This is because we do not take into account the small Balmer and Paschen discontinuities that should be present in the nebular continua due to dust scattered light from the Trapezium stars (see O’Dell & Hubbard 1965). It is beyond the scope of this paper to estimate the corrections to the temperatures due to this fact, but considering the large uncertainties of the t^2 determinations based on the discontinuities, its effect in the finally adopted weighted mean value of t^2 must be certainly negligible.

We have calculated the weighted mean of the t^2 values given in Table 12 to get a t^2 representative of the observed zone of the Orion nebula. The final adopted value is $t^2 = 0.022 \pm 0.002$. This result is consistent with those obtained by EPTE for the same zone: $t^2 = 0.028 \pm 0.07$, and their nearby Position 1: $t^2 = 0.020 \pm 0.07$. In addition, Rubin et al. (1998) obtained an independent determination of $t^2 = 0.032$ from the comparison of the N^+/O^+ ratios de-

Table 13. Adopted ICF values.

Element	Unseen ion	Value
He	He^0	1.12
C	C^+	1.20
N	N^{++}	5.68/5.90 ^a
Ne	Ne^+	1.60
S	S^{3+}	1.10
Ar	Ar^+	1.33
Fe	Fe^+	1.07
Fe	Fe^+, Fe^{++}	4.96/5.14 ^a

^a Values for $t^2=0.000/t^2=0.022$

rived from optical and ultraviolet (UV) lines taken from the combination of *Hubble Space Telescope* (HST) UV spectra of three zones of the Orion nebula. Finally, in a recent paper, O’Dell, Peimbert & Peimbert (2003) have obtained a direct estimation of t^2 from the spatial changes in a high spatial resolution map (obtained from HST images) columnar electron temperature of a region to the southwest of the Trapezium in the Orion nebula, very near our slit position. Their value is $t^2 = 0.028 \pm 0.006$. As it can be seen, it is very encouraging that different independent methods provide very consistent results, this suggest that temperature fluctuations are likely to be present in Orion nebula and that the true representative t^2 of its central parts should be between 0.020-0.030.

9 TOTAL ABUNDANCES

We have to adopt a set of ionization correction factors, ICFs, to correct for the unseen ionization stages in order to derive the total gaseous abundances of the different chemical elements. In our case, we adopt the ICF scheme used by EPTE for all the elements except Fe. For this element, we have determined the total abundance using two different ICFs. Firstly, we have considered our Fe^{++} abundance and the ICF proposed by Rodríguez & Rubin (2004):

$$\frac{N(\text{Fe})}{N(\text{H})} = \left[\frac{N(O^+)}{N(O^{++})} \right]^{0.09} \times \frac{N(\text{Fe}^{++})}{N(O^+)} \times \frac{N(O)}{N(\text{H})}. \quad (2)$$

Secondly, we have added our Fe^{++} and Fe^{3+} abundances and include an ICF for the contribution of Fe^+ . This contribution has been estimated from the observations of Rodríguez (2002), who determine the Fe^+ abundance from the $[\text{Fe II}] \lambda 8617 \text{ \AA}$ line. We have considered a $Fe^+/Fe^{++}=0.20$, the average of the ratios obtained by Rodríguez (2002) for her four slit positions nearer the Trapezium cluster. The values of the ICFs assumed for the different chemical elements are included in Table 13.

In Table 14 we show the total abundances obtained for our slit position of the Orion nebula. We include two different sets of abundances, one assuming no temperature fluctuations ($t^2 = 0$) and a second one using our final adopted value of $t^2 = 0.022 \pm 0.002$. In the table, we also compare with the abundances obtained by EPTE for their slit position 2, which coincides with our observed zone. We can see that the abundances are fairly similar in both set of data. Only Ne and Ar show differences larger than 0.1 dex. In the case of O we have included three sets of values: that obtained

Table 14. Total abundances^a.

Element	This Work		EPTE (Pos. 2)	
	$t^2=0.000$	$t^2=0.022\pm 0.002$	$t^2=0.000$	$t^2=0.028$
He	10.991±0.003	10.988±0.003	11.00	10.99
C ^b	8.42±0.02	8.42±0.02	8.37	8.37
N	7.65±0.09	7.73±0.09	7.60	7.78
O	8.51±0.03	8.67±0.04	8.47	8.65
O ^b	8.71±0.03	8.71±0.03
O ^c	8.63±0.03	8.65±0.03	...	8.68
Ne	7.78±0.07	8.05±0.07	7.69	7.89
Ne ^b	8.16±0.09	8.16±0.09
S	7.06±0.04	7.22±0.04	7.01	7.24
Cl	5.33±0.04	5.46±0.04	5.17	5.37
Ar	6.50±0.05	6.62±0.05	6.53	6.86
Fe ^d	6.07±0.08	6.23±0.08
Fe ^e	5.86±0.10	5.99±0.10
Fe ^f	6.27	6.34
Fe ^g	6.01	6.07

^a In units of $12+\log(X^m/H^+)$.

^b Value derived from RLs.

^c Value derived from O II RLs and [O II] CELs.

^d Assuming $ICF(Fe^++Fe^{3+})$.

^e Assuming $ICF(Fe^+)$.

^f From Fe^++Fe^{++} and assuming $ICF(Fe^{3+})$.

^g From $Fe^++Fe^{++}+Fe^{3+}$.

only from CELs, that obtained only from RLs and a last one that includes O^{++}/H^+ obtained from RLs and O^+/H^+ obtained from CELs. We prefer this last determination because the O^+/H^+ ratio determined from RLs is based on a single faint line located in a spectral zone with strong and numerous sky emission lines (see Sect. 7). In the case of N, as it was commented in Sect. 7, we do not have considered the N^{++} abundance obtained from RLs because it gives abnormally large values of the final N/H ratio: $12+\log(N/H) = 8.32\pm 0.02$ (for any of the two values of t^2 considered). This indicates that the observed N II lines are not produced by pure recombination and an important contribution by fluorescence should be present. Finally, in the case of Fe, we find a ratio of about 1.9 in the two values of the Fe abundance given in Table 14. Rodríguez (2003) finds a similar result when comparing the Fe abundances of several objects. This author indicates that the most likely explanation of this discrepancy is that either the collision strengths of [Fe IV] or the Fe ionization fractions predicted by ionization models (used for constructing Eq. 2) are unreliable. Unfortunately, we can not distinguish between these two possibilities.

10 DISCUSSION

The Orion nebula is traditionally considered the standard reference for the chemical composition of the ionized gas in the solar neighborhood. Therefore, it is essential to have a confident determination of elemental abundances for this object. Until very recently it was thought that the Sun was a chemical anomaly because of its large abundances –specially O– with respect to other nearby objects including the Orion nebula. In fact, at the beginning of the 90s the difference between the oxygen abundance of the Sun and the Orion nebula was about +0.4 dex (comparing the solar abundances of

Grevesse & Anders 1989 and those of the Orion nebula of Osterbrock et al. 1992). The recent corrections to the solar O abundance by Asplund et al. (2004) have lowered it by a factor of 0.2 dex. On the other hand, our Orion nebula determinations based on RLs give also O/H ratios higher than the older ones by Osterbrock et al. (1992). However, for a correct comparison between solar and ionized gas abundances we have to correct for the fraction of heavy elements embedded in dust grains in the nebula. EPTE estimated that C and O abundances in Orion nebula should be depleted onto dust grains by factors of 0.10 dex and 0.08 dex, respectively. Adding this factors to the gaseous abundances we have appropriate values to comparing with the solar ones. In the cases of N, S and Cl, no dust correction is applied since they are not significantly depleted in the neutral interstellar medium (Savage & Sembach 1996). For He, Ne and Ar, no correction is necessary because they are noble gases. In Table 15 we compare our Orion nebula gas+dust abundances –corrected for depletion onto dust grains– with those of the Sun, young F–G disk stars (ages ≤ 2 Gyr), nearby B dwarfs and gas-phase abundances of the local diffuse clouds. For the Sun: He comes from Christensen-Dalsgaard (1998); C and N from Asplund (2003); O, Ne and Ar from Asplund et al. (2004), and S and Cl from Grevesse & Sauval (1998). The data for F–G and B stars have been taken from the compilations by Sofia & Meyer (2001) and Herrero (2003), respectively. The interstellar standard abundances of the nearby diffuse clouds have been taken from Sofia & Meyer (2001).

The comparison of abundances given in Table 15 is very interesting. The O/H ratio of the Orion nebula is slightly higher but basically consistent within the uncertainties with the O abundance of young F–G stars, B dwarfs and the Sun. This is a certainly remarkable result that does not longer support previous thoughts about the abnormally high chemical composition of the Sun with respect to other objects of the solar vicinity. In the case of C, the abundance is similar to that of F–G stars, somewhat higher than in the Sun and considerably higher than in B dwarfs. Nevertheless, the C abundance of B dwarfs could be erroneous because it could be affected by NLTE effects or problems with the C atomic model used as it has been pointed out by Herrero (2003). The N abundance of the Orion nebula is somewhat lower than in B dwarfs and the Sun, but consistent within the uncertainties. In the case of the other elements: Ne, S, Cl and Ar we can only compare with the Sun and their abundances are rather consistent except in the cases of Ne and Ar for which the differences are higher than 0.2 dex. Similar large differences for these elements are also reported in our data for the H II region NGC 3576 (García-Rojas et al. 2004). This indicates that those differences are not spurious but we cannot ascertain the exact reason for the discrepancy.

The comparison with the abundances of nearby diffuse clouds is specially revealing. It is expected that C and O should be depleted onto dust grains in diffuse clouds (e.g. Jenkins 1987) and most probably in a larger amount than in ionized nebulae, where some dust destruction seems to operate (e.g. Rodríguez 1996). In this sense, the abundances obtained for diffuse clouds should be considered as lower limits of the expected ones in H II regions. It is important to indicate that the comparison between the C and O abundances in diffuse clouds and those we obtain from CELs and assuming $t^2=0.000$ for the Orion nebula –8.02 and 8.51 for

Table 15. Chemical composition of different objects of the solar vicinity^a.

Element	Orion gas+dust	Neutral ISM ^b	Young F and G stars ^b	B dwarfs ^c	Sun ^d	Orion–Sun
He	10.988±0.003	10.98±0.02	+0.008
C	8.52±0.02	8.15±0.06	8.55±0.10	8.25±0.08	8.41±0.05	+0.11
N	7.73±0.09	7.81±0.09	7.80±0.05	−0.07
O	8.73±0.03	8.50±0.02	8.65±0.15	8.68±0.06	8.66±0.05	+0.07
Ne	8.05±0.07	7.84±0.06	+0.21
S	7.22±0.04	7.20±0.08	+0.02
Cl	5.46±0.04	5.28±0.08	+0.18
Ar	6.62±0.05	6.18±0.08	+0.44

^a In units of $12+\log(X^m/H^+)$.

^b Sofia & Meyer (2001).

^c Herrero (2003).

^d Christensen-Dalsgaard (1998); Grevesse & Sauval (1998); Asplund (2003); Asplund et al. (2004).

C and O, respectively– do not give room for the expected dust destruction that should occur in ionized nebulae. The higher C and O abundances obtained from RLs –or from CELs assuming an appropriate t^2 – are more consistent with what is expected by the dust destruction scheme.

The last column of Table 15 gives the difference between our Orion nebula abundances and the Solar ones. We find that most of the heavy elements give a positive difference, with an average value of about +0.09 dex (average of the element values of Table 15 except He and Ar). This difference is in agreement with the estimations of the chemical evolution models by Carigi (2003) and Akerman et al. (2004) who found that the O/H ratio at the solar galactocentric distance has increased by 0.12 dex since the Sun was formed.

Fe has not been included in Table 15 because large dust depletion factors are expected for this element in ionized nebulae. EPTE estimated a depletion of 1.37 dex comparing their gaseous Fe/H ratio with that of 7.48 ± 0.15 derived from B stars of the Orion association by Cunha & Lambert (1994). If we consider this last value as representative of the gas+dust Fe abundance of the Orion nebula, we obtain depletion factors of 1.25 and 1.49 dex depending on the final ICF scheme adopted to obtain the gaseous Fe/H ratio.

11 CONCLUSIONS

We present echelle spectroscopy in the 3100–10400 Å range for the Orion nebula for a slit position coincident with previous observations of Peimbert & Torres-Peimbert (1977) and EPTE. We have measured the intensity of 555 emission lines. This is the most complete list of emission lines ever obtained for this relevant object, and the largest collection of emission lines available for a Galactic or extragalactic H II region.

We have derived the physical conditions of the nebula making use of many different line intensities and continuum ratios. The chemical abundances have been derived making use of collisionally excited lines for a large number of ions as well as recombination lines for He⁺, C⁺⁺, O⁺, O⁺⁺ and Ne⁺⁺. In the case of O⁺ and Ne⁺⁺ this is the first time that their abundance is derived from recombination lines. We have determined C⁺⁺ and O⁺⁺ abundances from several lines corresponding to $f-d$ transitions that have not been observed in previous works. The abundances

obtained from recombination lines are always larger than those derived from collisionally excited lines for all the ions where both kinds of lines are measured. We obtain remarkably consistent independent estimations of the temperature fluctuation parameter derived from different methods, which adopted average value is $t^2 = 0.022\pm 0.002$, similar to other estimates from the literature. This result strongly suggests that moderate temperature fluctuations are present in the Orion nebula.

The Orion nebula is a standard reference for the chemical composition of the ionized gas of the solar vicinity and, therefore, it is important to have a confident set of abundances for this object in order to improve our knowledge of the chemical evolution of this particular zone of the Galaxy. We have compared the chemical composition of the nebula with that of the Sun and other representative objects, as the neutral diffuse ISM, young F and G stars and B dwarfs of the solar vicinity. The abundances of the heavy elements in the Orion nebula are only slightly higher –about 0.09 dex– than the solar ones, a difference that can be explained by the chemical evolution of the solar vicinity since the Sun was formed. The recent corrections to the solar abundances and our new values of the gas+dust Orion nebula abundances seem finally to converge, washing out the long-standing problem of the apparently abnormal solar abundances.

ACKNOWLEDGMENTS

We would like to thank R. Kisielius and P. J. Storey for providing us with their latest calculations of effective recombination coefficients for Ne and D. P. Smits for providing us unpublished atomic calculations for He. CE and JG would like to thank the members of the Instituto de Astronomía, UNAM, for their always warm hospitality. This work has been partially funded by the Spanish Ministerio de Ciencia y Tecnología (MCyT) under project AYA2001-0436. MP received partial support from DGAPA UNAM (grant IN114601). MTR received partial support from FONDAP(15010003), a Guggenheim Fellowship and Fondecyt(1010404). MR acknowledges support from Mexican CONACYT project J37680-E.

REFERENCES

- Akerman C. J., Carigi L., Nissen P. E., Pettini M., Asplund M., 2004, *A&A*, 414, 931
- Asplund M., 2003 in Charbonnel C., Schaerer D., Meynet G., eds, *ASP Conf. Ser. Vol. 304, CNO in the Universe*. Astron. Soc. Pac., San Francisco, 275
- Asplund M., Grevesse N., Sauval A.J., Allende-Prieto C., Kiselman D., 2004, *A&A*, 417, 751
- Baldwin J. A., Ferland G. J., Martin P. G., Corbin M. R., Cota S. A., Peterson B. M., Slettebak A., 1991, *ApJ*, 374, 580
- Baldwin J. A., Verner E. M., Verner D. A., Ferland G. J., Martin P. G., Korista K. T., Rubin R.H., 2000, *ApJ*, 129, 229
- Benjamin R. A., Skillman E. D., Smits D. P., 1999, *ApJ* 514, 307
- Benjamin R. A., Skillman E. D., Smits D. P., 2002, *ApJ* 569, 288
- Brown R. L., Mathews W. G., 1970, *ApJ*, 160, 939
- Christensen-Dalsgaard J., 1998, *Space Sci. Rev.*, 85, 19
- Carigi L., 2003, *MNRAS*, 339, 825
- Costero R., Peimbert M., 1970, *Bol. Obs. Tonantzintla y Tacubaya*, 5, 229
- Cunha K., Lambert D. L., 1994, *ApJ*, 426, 170
- Davey A. R., Storey P. J., Kisielius R., 2000, *A&AS*, 142, 85
- De Robertis M. M., Dufour R. J., Hunt R. W., 1987, *J. Roy. Astron. Soc. Can.*, 81, 195
- D'Odorico S., Cristiani S., Dekker H., Hill V., Kaufer A., Kim T., Primas F., 2000, *Proc. SPIE*, 4005, 121
- Escalante V., Victor G. A., 1990, *ApJS*, 73, 513
- Escalante V., Victor G. A., 1992, *Planet. Space Sci.*, 40, 1705
- Esteban C., 2002, *Rev. Mex. Astron. Astrofs. Ser. Conf.*, 12, 56
- Esteban C., Peimbert M., Torres-Peimbert S., Escalante V. 1998, *MNRAS*, 295, 401
- Esteban C., Peimbert M., Torres-Peimbert S., García-Rojas J., 1999a, *Rev. Mex. Astron. Astrofs.*, 35, 65
- Esteban C., Peimbert M., Torres-Peimbert S., García-Rojas J., Rodríguez M., 1999b, *ApJS*, 120, 113
- Esteban C., Peimbert M., Torres-Peimbert S., Rodríguez M., 2002, *ApJ*, 581, 241
- Ferland G. J., 2001, *PASP*, 113, 41
- Froese Fischer C., Rubin R. H., 1998, *J. Phys. B: At. Mol. Opt. Phys.*, 31, 1657
- García-Rojas J., Esteban C., Peimbert M., Rodríguez M., Ruiz M. T., Peimbert A., 2004a, *ApJS*, in press (astro-ph/0404123)
- Garstang R. H., 1958, *MNRAS*, 118, 572
- Grandi, S. A., 1976, *ApJ*, 206, 658
- Grandi, S. A., 1975a, *ApJ*, 196, 465
- Grandi, S. A., 1975b, *ApJ*, 196, L43
- Grevesse N., Sauval A. J., 1998, *Space Sci. Rev.*, 85, 161
- Herrero A., 2003 in Charbonnel C., Schaerer D., Meynet G., eds, *ASP Conf. Ser. Vol. 304, CNO in the Universe*. Astron. Soc. Pac., San Francisco, 10
- Jenkins E. B., 1987, in Hollenbach D.J., Thronson H. A., eds, *Interstellar Processes*, Reidel, Dordrecht, 533
- Kaler J. B., Aller L. H., Bowen I. S., 1965, *ApJ*, 141, 912
- Kingdon J., Ferland G., 1995, *ApJ* 442, 714
- Kisielius R., Storey P. J., 2002, *A&A*, 387, 1135
- Kisielius R., Storey P. J., Davey A. R., Neale L. T., 1998, *A&AS*, 133, 257
- Lester D. F., Dinerstein H. L., Rank D. M., 1979, *ApJ* 232, 139
- Liu X.-W., 2002, *Rev. Mex. Astron. Astrofs. Ser. Conf.*, 12, 70
- Liu X.-W., 2003, in Sutherland R., Kwok S., Dopita M. A., eds, *Proc. IAU Symp. 209, Planetary Nebulae*. Astron. Soc. Pac., San Francisco, in press
- Liu X.-W., Storey P. J., Barlow M. J., Clegg R. E. S., 1995, *MNRAS*, 272, 369
- Liu X.-W., Storey P. J., Barlow M. J., Danziger I. J., Cohen M., & Bryce M., 2000, *MNRAS*, 312, 585
- Mathis J. S., Liu X.-W., 1999, *ApJ*, 521, 212
- McLaughlin B. M., Bell K.L., 1993, *ApJ*, 408, 753
- Mendoza C., 1983, in Flower D. R., Reidel D., eds, *Proc. IAU Symp. 103, Planetary Nebulae*, Kluwer, Dordrecht, 143
- Moore C. E., 1945, *A Multiplet Table of Astrophysical Interest*. *Contrib. Princeton Univ. Obs.*, 20.
- Moore C. E., 1993, *Tables of Spectra of Hydrogen, Carbon, Nitrogen and Oxygen Atoms and Ions*. CRC Press, Inc. Boca Raton
- Nussbaumer H., Storey P.J., 1984, *A&AS*, 56, 293
- O'Dell C. R., 2001, *PASP*, 113, 29
- O'Dell C. R., Hubbard W. B., 1965, *ApJ*, 142, 591
- O'Dell C. R., Peimbert M., Peimbert A., 2003, *AJ*, 125, 2590
- Osterbrock D. E., Tran H. D., Veilleux S., 1992, *ApJ*, 389, 196
- Peimbert A., 2003, *ApJ*, 584, 735
- Peimbert A., Peimbert M., Luridiana V., 2002, *ApJ*, 565, 668
- Peimbert M., 1967, *ApJ*, 150, 825
- Peimbert M., Costero R., 1969, *Bol. Obs. Tonantzintla y Tacubaya*, 5, 3
- Peimbert M., Peimbert A., Ruiz M. T., 2000, *ApJ*, 541, 688
- Peimbert M., Peimbert A., Ruiz M. T., Esteban C., 2004, *ApJS* 150, 431
- Peimbert M., Storey P. J., Torres-Peimbert S., 1993, *ApJ*, 414, 626
- Peimbert M., Torres-Peimbert S., 1977, *MNRAS*, 179, 217
- Péquignot, D., Petitjean, P., & Boisson, C. 1991, *A&A*, 251, 680
- Pradhan A. K., 1976, *MNRAS*, 177, 31
- Quinet P., 1996, *A&AS*, 116, 573
- Rodríguez M., 1996, *A&A*, 313, L5
- Rodríguez M., 1999, *A&A*, 348, 222
- Rodríguez M., 2002, *A&A*, 389, 556
- Rodríguez M., 2003, *ApJ*, 590, 296
- Rodríguez M., Rubin R.H., 2004, in Duc P.-A., Braine J., Brinks E., eds, *Proc. IAU Symp. 217, Recycling Inter-galactic and Interstellar Matter*. Astron. Soc. Pac., San Francisco, in press
- Rola C., Stasińska G., 1994, *A&A*, 282, 199
- Rubin R., Martin P. G., Dufour R. J., Ferland G. F., Baldwin J. A., Hester J. J., Walter D. K., 1998, *ApJ*, 495, 891
- Rubin R., Simpson J. P., Haas M. R., Erickson E. F., 1991, *ApJ* 364, 564
- Savage B. D., Sembach K. R., 1996, *ApJ*, 457, 211

Sawey P. M. J., Berrington K. A., 1993, *Atomic Data Nucl. Data Tables*, 55, 81
 Sharpee B., Williams R., Baldwin J. A., van Hoof P. A. M., 2003, *ApJS*, 149, 157
 Shaw R. A., & Dufour, R. J. D. 1995, *PASP*, 107, 896
 Smits D. P., 1996, *MNRAS*, 278, 683
 Sofia U. J., Meyer D. M., 2001, *ApJ*, 554, L221
 Stasińska G., 2002, *Rev. Mex. Astron. Astrofis. Ser. Conf.*, 12, 62
 Storey P.J., 1994, *A&A*, 282, 999
 Storey P.J., Hummer D.G., 1995, *MNRAS*, 272, 41
 Torres-Peimbert S., Peimbert M., 2003, in Kwok S., Dopita M. A., Sutherland R., eds, *Proc. IAU Symp. 209, Planetary Nebulae. Astron. Soc. Pac., San Francisco*, 363
 Torres-Peimbert S., Peimbert M., Daltabuit E., 1980, *ApJ*, 238, 133
 Tsamis Y. G., Barlow M. J., Liu X.-W., Danziger I. J., Storey P. J., 2003, *MNRAS*, 338, 687
 Verner, E. M., Verner, D. A., Baldwin, J. A., Ferland, G. J., Martin, P. G., 2000, *ApJ*, 543, 831
 Walter D. K., Dufour R. J., Hester J. J., 1992, *ApJ*, 397, 196
 Wiese W. L., Fuhr J. R., Deters T. M., 1996, *Journal of Physical and Chemical Reference Data, Monograph No. 7, Atomic Transition Probabilities of Carbon, Nitrogen and Oxygen. American Chemical Society and American Institute of Physics.*
 Wiese W. L., Smith M. W., Glennon B. M., 1966, *Atomic Transition Probabilities: Volume I: Hydrogen Through Neon: A critical Data Compilation, National Bureau of Standards, NBS 4. Washington*
 Zeppen C. J., 1982, *MNRAS*, 198, 111
 Zhang H. L., 1996, *A&AS*, 119, 523
 Zhang H. L., Pradhan A. K., 1997, *A&AS*, 126, 373

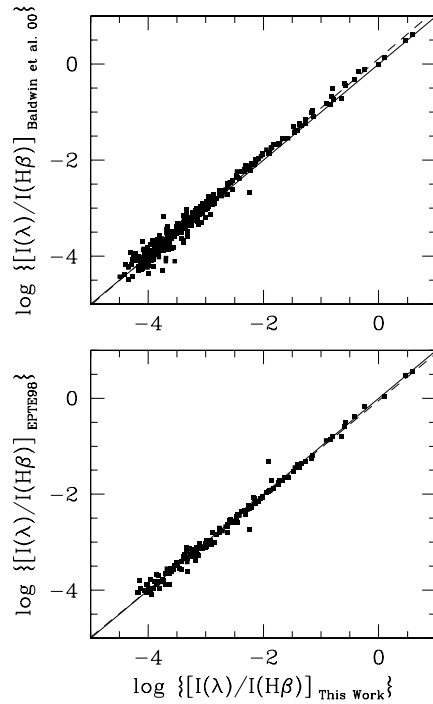


Figure 1. Comparison of line intensity ratios from this work with those of Baldwin et al. 2000 (top) and Esteban et al. 1998 (bottom). Continuous line represents the ideal relation with a slope of 1. Discontinuous line corresponds to the linear least-squares fit of the line ratios.

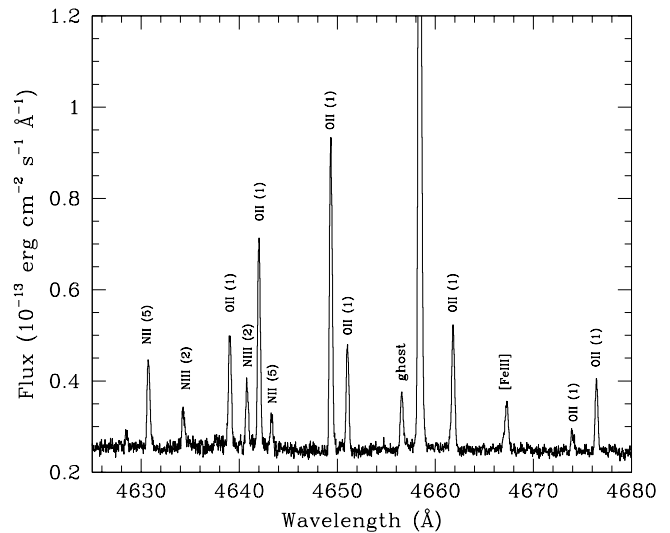


Figure 2. Section of the echelle spectrum showing all the individual emission lines of multiplet 1 of O II (observed fluxes).

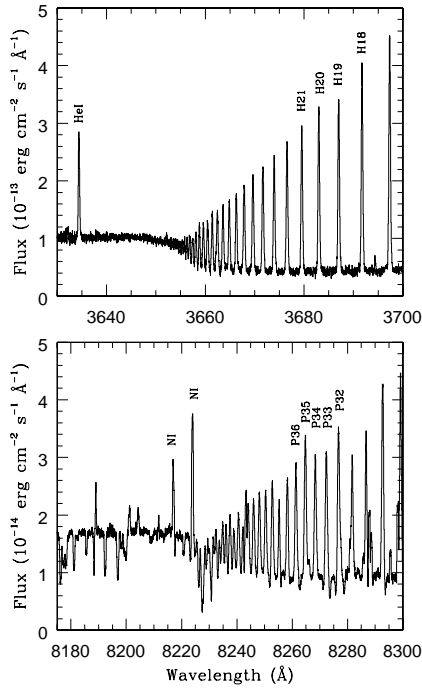


Figure 3. Section of the echelle spectrum showing the Balmer (top) and Paschen (bottom) discontinuities (observed fluxes).

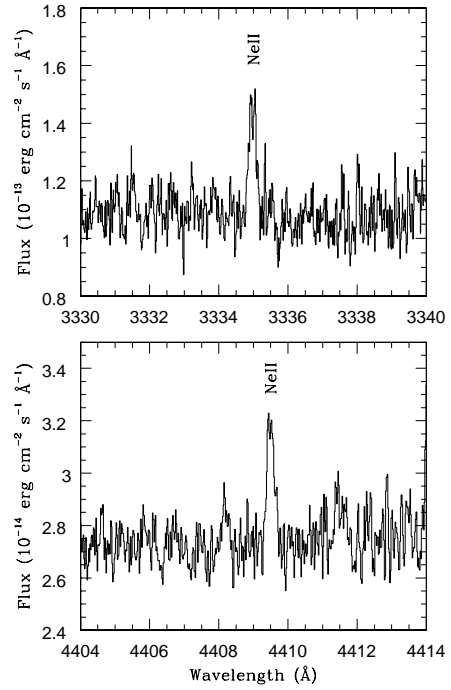


Figure 5. Section of the echelle spectrum showing some of the pure recombination Ne II lines detected (observed fluxes).

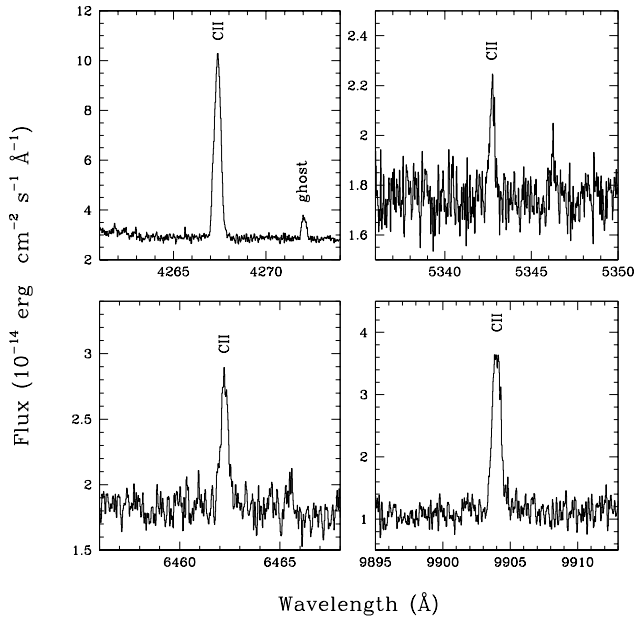


Figure 4. Section of the echelle spectrum showing some of the pure recombination C II lines detected (observed fluxes).